

Two-point correlators in non-conformal $\mathcal{N} = 2$ gauge theories

M. Billò,^a F. Fucito,^b G.P. Korchemsky,^c A. Lerda^d and J. F. Morales^b

^a*Università di Torino, Dipartimento di Fisica and I. N. F. N. - sezione di Torino,
Via P. Giuria 1, I-10125 Torino, Italy*

^b*I. N. F. N. - sezione di Roma Tor Vergata
Via della Ricerca Scientifica, I-00133 Roma, Italy*

^c*Institut de Physique Théorique¹, Université Paris Saclay, CNRS, CEA, 91191 Gif-sur-Yvette*

^d*Università del Piemonte Orientale, Dipartimento di Scienze e Innovazione Tecnologica
and I. N. F. N. - sezione di Torino, Via P. Giuria 1, I-10125 Torino, Italy*

E-mail: billò@to.infn.it, fucito@roma2.infn.it,
gregory.korchemsky@ipht.fr, lerda@to.infn.it, morales@roma2.infn.it

ABSTRACT: We study the two-point correlation functions of chiral/anti-chiral operators in $\mathcal{N} = 2$ supersymmetric Yang-Mills theories on \mathbb{R}^4 with gauge group $SU(N)$ and N_f massless hypermultiplets in the fundamental representation. We compute them in perturbation theory, using dimensional regularization up to two loops, and show that field-theory observables built out of dimensionless ratios of two-point renormalized correlators on \mathbb{R}^4 are in perfect agreement with the same quantities computed using localization on the four-sphere, even in the non-conformal case $N_f \neq 2N$.

KEYWORDS: $\mathcal{N} = 2$ SYM theories, matrix models, correlation functions

In memoriam of our collaborator and friend Yassen Stanislavov Stanev

¹Unité Mixte de Recherche 3681 du CNRS

Contents

1	Introduction	2
2	Two-point correlators from perturbation theory	4
2.1	Tree-level	7
2.2	One-loop diagrams	7
2.3	Two-loop diagrams	9
2.3.1	$v_{2,1}^2$ - contributions	9
2.3.2	$v_{2,2}$ - and $v_{4,2}$ - contributions	10
2.4	Effective vertices	13
2.5	Summary of results	16
3	Renormalization	17
3.1	The β -function and anomalous dimensions	18
3.2	Renormalized correlators	20
3.3	Normalized correlators	21
4	Matrix model approach	23
4.1	Chiral and anti-chiral operators in the matrix model	25
4.2	Correlators in the matrix model	26
4.3	Comparison between matrix model and field theory correlators	27
5	Two-point correlators on the four-sphere	28
6	Summary and conclusions	32
A	Loop integrals	33
A.1	Triangle identity	33
A.2	Scalar integrals	34
B	Evaluation of the relevant (super)diagrams	37
B.1	Feynman rules	37
B.2	One-loop diagrams	39
B.3	Two-loop diagrams	40
C	Feynman integral on the sphere	52

1 Introduction

Supersymmetric Yang-Mills theories (SYM) have long been considered as an ideal playground to get exact results in Quantum Field Theory. In recent times, exact formulae for special observables in theories with extended supersymmetries have been found. In four-dimensional theories with maximal $\mathcal{N} = 4$ supersymmetry, the exact resummation of the infinite series of perturbative corrections to the expectation value of circular Wilson loops, also in presence of chiral operators, has been performed [1–5]. These results are based on the counting of the relevant rainbow-like Feynman diagrams by means of a matrix model. The introduction of this matrix model has been considered *ad hoc* until it was shown [6] that localization for the $\mathcal{N} = 2^*$ theory on the four-sphere S^4 , after having performed the $\mathcal{N} = 4$ limit, predicts its existence. Moreover, localization provides a non-perturbative formula for the circular Wilson loop in a general $\mathcal{N} = 2$ theory which takes into account both perturbative and non-perturbative, instanton and anti-instanton, corrections in an interacting matrix model. A two-loop test of this formula against perturbation theory was presented in [7] in the case of superconformal QCD.

It is natural to ask whether localization on S^4 can be used to compute non-trivial quantities other than the Wilson loop expectation value. In [8–14] it has been proposed that two-point correlators between chiral and anti-chiral operators in a superconformal $\mathcal{N} = 2$ theory on \mathbb{R}^4 can be computed from the partition function of the theory on the four-sphere with chiral and anti-chiral insertions at the north and south pole respectively; localization expresses this partition function as a matrix model. In a conformal $\mathcal{N} = 2$ theory, two-point correlators between a chiral operator $O_{\vec{n}} = \text{tr}(\varphi^{n_1})\text{tr}(\varphi^{n_2})\cdots$, where $\vec{n} = (n_1, n_2, \dots)$ and φ is the complex scalar of the gauge vector multiplet, and an anti-chiral operator $\bar{O}_{\vec{m}}$ made out of the complex conjugate field $\bar{\varphi}$, take the form

$$\langle O_{\vec{n}}(x) \bar{O}_{\vec{m}}(0) \rangle = \frac{G_{\vec{n}, \vec{m}}(g_0)}{(4\pi^2 x^2)^n} \delta_{n, m}, \quad (1.1)$$

where $n = \sum_i n_i$ and $m = \sum_j m_j$ are the scaling dimensions of the two operators. $G_{\vec{n}, \vec{m}}(g_0)$ is a non-trivial function of the coupling constant g_0 , but bears no dependence on the distance x since chiral and anti-chiral operators are protected in conformal $\mathcal{N} = 2$ theory. The two-point functions on a four-sphere also take the form (1.1) but with x^2 being the chordal distance on S^4 . The function $G_{\vec{n}, \vec{m}}(g_0)$ is the same on the sphere and in flat space, and it is given by a two-point function in a matrix model obtained from localization.

Explicit tests of the match between the field theory and the matrix model descriptions of the correlator (1.1) have been performed up to two loops for low-dimensional operators in $\text{SU}(2)$ and $\text{SU}(3)$ gauge theories with $N_f = 4$ and $N_f = 6$ matter hypermultiplets. The results were extended in [15] to generic chiral operators in a superconformal $\text{SU}(N)$ theory with $N_f = 2N$. Also the one-point functions of chiral operators in presence of a circular Wilson loop can be expressed in terms of the matrix model obtained via localization of the Wilson loop on S^4 , as checked up to two loops in [16].

It is of obvious importance to investigate to what extent the matrix model description of the correlation function persists in $\mathcal{N} = 2$ theory in non-conformal set-ups. A first step

in this direction was carried out in [15] for a $SU(N)$ theory with N_f flavors, where suitable operators were chosen in such a way that their two-point correlators vanish in perturbation theory up to a given loop order, leaving a finite contribution at the next leading loop order. In such a situation, a perfect match between the perturbation theory and localization was shown for an arbitrary rank and any number of flavors at two and three loops. This strongly hints that chiral/anti-chiral correlators are related to the S^4 matrix model also beyond the conformal case.

Considering generic chiral/anti-chiral correlation functions away from the conformal point $N_f = 2N$, we encounter important differences. For $N_f \neq 2N$, the gauge coupling and the operators are not anymore protected from quantum corrections and have to be renormalized to account for the ultraviolet (UV) divergences. As a consequence, the two-point correlation functions of renormalized operators $O_{\vec{n}}^R$ and $\bar{O}_{\vec{m}}^R$ depend on the renormalization scale μ and are no longer forced to have just a power-like dependence on the distance x as in (1.1). Instead, they take the general form

$$\langle O_{\vec{n}}^R(x) \bar{O}_{\vec{m}}^R(0) \rangle = \frac{G_{\vec{n},\vec{m}}^R(g, \nu)}{(4\pi^2 x^2)^n} \delta_{n,m} , \quad (1.2)$$

where $g = g(\mu)$ is the renormalized coupling and the dimensionless quantity

$$\nu = 2 + \gamma_E + \ln \pi \mu^2 x^2 \quad (1.3)$$

parametrizes the distance separation. Here γ_E denotes the Euler-Mascheroni constant. In contrast to the conformal case, the function $G_{\vec{n},\vec{m}}^R(g, \nu)$ depends non-trivially on the distance x^2 through the quantity ν . Such a dependence cannot be obtained from localization on S^4 , because in this case the operators are inserted at the opposite poles of the four-sphere and the distance between them is fixed in terms of the sphere radius. Still our results show that, up to two loops, the ν -dependence is very simple and can be put in the factorized form

$$G_{\vec{n},\vec{m}}^R(g, \nu) = \frac{G_{\vec{n},\vec{m}}^R(g, 0)}{(1 + \frac{1}{2}\beta_0 g^2 \nu)^n} \delta_{nm} + O(g^6) , \quad (1.4)$$

where β_0 is the expansion coefficient of the exact one-loop β -function of the theory, namely

$$\beta_0 = \frac{N_f - 2N}{8\pi^2} . \quad (1.5)$$

Remarkably, the ν -dependent prefactor in (1.4) depends only on the scaling dimension n and not on the details of the operators. As a consequence, up to two loops at least, ratios of correlators of the same scaling dimension are actually ν -independent and can be compared directly against the matrix model results. We show that the field theory results for such observables are indeed in perfect agreement with the predictions from the localization matrix model. This is consistent with the fact that all Feynman diagrams contributing to the ratios are finite in four dimensions, and finite loop integrals on S^4 and \mathbb{R}^4 yield the same result after replacing propagators in flat space by those on the four-sphere, as we will show in Section 5.

Furthermore, one can ask whether the results for the renormalized correlators at a given renormalization scale can be directly matched against those coming from localization. At one loop, we show that this is indeed the case if we choose $\mu^2 x^2 = e^{\gamma_E}/\pi$ in the minimal subtraction scheme. Moreover, by considering the field theory on S^D and evaluating the relevant one-loop integrals in dimensional regularization, we find that, apart from the obvious replacement of propagators, not only the divergent parts but also the finite parts agree with the results on \mathbb{R}^D for $D \rightarrow 4$. While the agreement of the divergent part is expected, since the divergences are sensible to short distances and do not distinguish between the sphere and flat space, the agreement of the finite part is neither expected nor guaranteed *a priori*, but nevertheless it holds. At two loops, we find that the matrix model results reproduce the field theory ones, up to a term proportional to $(2N - N_f)$ and to the dimension n of the operators. This suggests that the difference could be interpreted as a conformal anomaly which, in non-conformal theories, affects the correlation functions in going from the four-sphere to the flat space.

In this paper we keep the numbers of colors N and flavors N_f arbitrary and compute the two-point correlators for a general choice of chiral/anti-chiral operators. On the field theory side we do this at the two-loop level. We summarize our findings in Section 2 and give a detailed account of the Feynman diagram computations in Appendices A and B. To keep track of the various particles exchanged in the loops we use a superfield formalism. The loop integrals are evaluated using the integration methods pioneered in [17] (see also [18] for a review). In Section 3 we compute the renormalized correlators and their anomalous dimensions. Our results suggest that the anomalous dimensions $\gamma_{\vec{n},0}$ of the chiral operators are one-loop exact and are given by the simple formula $\gamma_{\vec{n},0} = \frac{n}{2} \beta_0$. In Section 4 we discuss the computation of the correlators on the matrix model side, building on the techniques described in [15], and compare the results with those previously obtained from the field theory side. To facilitate the comparison, we show that, up to two loops, the localization matrix model can be re-expressed as a complex matrix model encoding the color factors and the combinatorics of the Feynman diagrams that contribute to the chiral/anti-chiral correlators. Finally, in Section 5 we discuss the field theory calculation of the two-point correlators on the four-sphere S^4 , and in Section 6 we present our conclusions. Several technical details for such calculations are provided in Appendix C.

2 Two-point correlators from perturbation theory

We consider a $\mathcal{N} = 2$ SYM theory with gauge group $SU(N)$ and N_f hypermultiplets in the fundamental representation. For $N_f = 2N$ the theory is conformally invariant also at the quantum level. We denote by $\varphi(x)$ the complex scalar field of the $\mathcal{N} = 2$ vector multiplet which, in $\mathcal{N} = 1$ notation, is the lowest component of a chiral superfield Φ . In this theory a basis of chiral operators can be given in terms of the multi-trace operators

$$O_{\vec{n}}(x) = \text{tr} (\varphi^{n_1}(x)) \text{tr} (\varphi^{n_2}(x)) \dots \text{tr} (\varphi^{n_\ell}(x)) , \quad (2.1)$$

where $\vec{n} = (n_1, n_2, \dots, n_\ell)$. The scaling (bare) dimension of $O_{\vec{n}}(x)$ is

$$n = \sum_{k=1}^{\ell} n_k. \quad (2.2)$$

We expand the scalar field $\varphi(x) = \varphi^a(x) T^a$ over the $SU(N)$ generators T^a ($a = 1, \dots, N^2 - 1$) in the fundamental representation, normalized as

$$\text{tr}(T^a T^b) = \frac{1}{2} \delta_{ab}. \quad (2.3)$$

In terms of the components $\varphi^a(x)$, the operators (2.1) become

$$O_{\vec{n}}(x) = R_{\vec{n}}^{a_1 \dots a_n} \varphi^{a_1}(x) \dots \varphi^{a_n}(x), \quad (2.4)$$

where $R_{\vec{n}}^{a_1 \dots a_n}$ is a completely symmetric tensor¹. In an analogous way, we define the anti-chiral operators $\bar{O}_{\vec{m}}(x)$ using the complex conjugate field $\bar{\varphi}(x)$ instead of $\varphi(x)$.

We are interested in computing the two-point correlation functions

$$\langle O_{\vec{n}}(x) \bar{O}_{\vec{m}}(0) \rangle \quad (2.5)$$

in non-conformal $\mathcal{N} = 2$ theories using standard perturbative techniques. We perform our calculations at the origin of moduli space, where the scalar fields have vanishing vacuum expectation values. This is a preferred point in the sense that here the breaking of conformal invariance occurs only at the quantum level, as a consequence of the dimensional transmutation phenomenon. Therefore, this is the natural place in which to test whether the matrix model approach based on localization agrees with the standard perturbative field-theory calculations also in the non-conformal case. Unlike the $\mathcal{N} = 4$ theory where the correlators (2.5) are exact at tree-level, in $\mathcal{N} = 2$ theories they receive quantum corrections, starting from one loop for $N_f \neq 2N$ and from two loops in the conformal case $N_f = 2N$. Moreover, in the non-conformal theories, the loop integrals are UV divergent, in general, and need to be regularized. Here, we use the dimensional regularization taking the space-time dimension to be $D = 4 - 2\epsilon$. As a consequence, the bare gauge coupling constant, g_0 , becomes dimensionful.

In general, the bare two-point functions (2.5) take the form

$$\langle O_{\vec{n}}(x) \bar{O}_{\vec{m}}(0) \rangle = \Delta^n(x) G_{\vec{n}, \vec{m}}(g_0, \epsilon, x) \delta_{nm} \quad (2.6)$$

where $n = m$ is the common scaling dimension of the two operators, and

$$\Delta(x) = \int \frac{d^D k}{(2\pi)^D} \frac{e^{ik \cdot x}}{k^2} = \frac{\Gamma(1 - \epsilon)}{4\pi (\pi x^2)^{1 - \epsilon}}. \quad (2.7)$$

¹Explicitly,

$$R_{\vec{n}}^{a_1 \dots a_n} = \text{tr}(T^{(a_1} \dots T^{a_{n_1}}) \text{tr}(T^{a_{n_1+1}} \dots T^{a_{n_1+n_2}}) \dots \text{tr}(T^{a_{n_1+\dots+n_{\ell-1}+1}} \dots T^{a_n}))$$

where the indices are symmetrized with strength 1.

is the massless scalar propagator in D -dimensions. The correlator $G_{\vec{n},\vec{m}}(g_0,\epsilon,x)$ can be computed at weak coupling as an expansion in powers of g_0^2 . We refer to [15] for details on the Feynman rules that are needed to perform this calculation; they are summarized for convenience in Appendix B.

The diagrams which contribute to the two-point functions (2.5) up to order g_0^4 are schematically represented in Fig. 1.

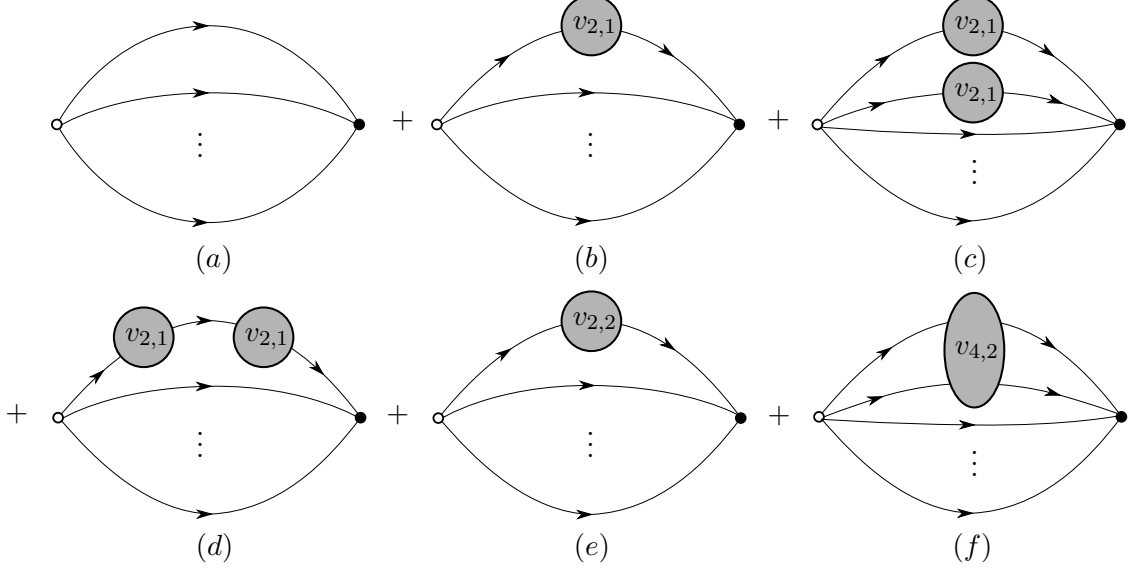


Figure 1. The Feynman diagrams contributing to the two-point correlators. White and black dots stand for the operators $O_{\vec{n}}$ and $\bar{O}_{\vec{m}}$, respectively. Lines with arrows denote free scalar propagators. The effective vertex $v_{k,\ell}$ represents the sum of irreducible diagrams with k external legs at ℓ loops.

The diagram (a) is the tree-level contribution, the diagram (b) is the one-loop correction, while the other four diagrams represent the two-loop part. The blobs labeled by $v_{k,\ell}$ stand for the sum of all irreducible diagrams of order $g_0^{2\ell}$ with k external lines - half of them connected to the chiral fields φ of $O_{\vec{n}}$, half to the anti-chiral ones of $\bar{O}_{\vec{m}}$.

A convenient way to organize the computation of these diagrams is to consider the $\mathcal{N} = 4$ theory, remove all contributions from Feynman diagrams involving loops of the adjoint hypermultiplet (which we call H) and add those with loops of the fundamental matter multiplets (which we call Q and \tilde{Q}) [7]. Since the two-point correlators in $\mathcal{N} = 4$ theory are exact at tree-level, we can write

$$\begin{aligned} G_{\vec{n},\vec{m}} &= G_{\vec{n},\vec{m}}|_{\mathcal{N}=4} - G_{\vec{n},\vec{m}}|_H + G_{\vec{n},\vec{m}}|_{Q,\tilde{Q}} \\ &= G_{\vec{n},\vec{m}}|_{\text{tree}} - G_{\vec{n},\vec{m}}|_H + G_{\vec{n},\vec{m}}|_{Q,\tilde{Q}} , \end{aligned} \quad (2.8)$$

where, in an obvious notation, $G_{\vec{n},\vec{m}}|_H$ stands for all diagrams in the $\mathcal{N} = 4$ theory with the adjoint hypermultiplet H circulating in the loops, and $G_{\vec{n},\vec{m}}|_{Q,\tilde{Q}}$ stands for the same diagrams in the $\mathcal{N} = 2$ theory with loops of fundamental matter multiplets Q and \tilde{Q} . In

the following, we will sometimes refer to this method as “performing the computation in the difference theory”. We stress that in the difference theory one should take into account only diagrams involving loops of the adjoint hypermultiplet or loops of the fundamental ones, but not both.

2.1 Tree-level

The tree-level contribution to the correlator (2.6) comes from the diagram in Fig. 1(a). To obtain its explicit expression, one contracts the fields φ in $O_{\vec{n}}$ with the fields $\bar{\varphi}$ in $\bar{O}_{\vec{m}}$ by means of a free scalar propagator

$$\langle \varphi^a(x) \bar{\varphi}^b(0) \rangle = \frac{a}{x} \longrightarrow \frac{b}{0} = \Delta(x) \delta^{ab}. \quad (2.9)$$

In this way one finds that the correlator $\langle O_{\vec{n}}(x) \bar{O}_{\vec{m}}(0) \rangle$ at tree-level takes the form (2.6) with

$$G_{\vec{n}, \vec{m}}|_{\text{tree}} = n! R_{\vec{n}}^{a_1 \dots a_n} R_{\vec{m}}^{a_1 \dots a_n} \quad (2.10)$$

being a constant that is determined by the color structure of the two operators. For example, for the first operators of even dimension, one finds [15]

$$\begin{aligned} G_{(2),(2)}|_{\text{tree}} &= \frac{N^2 - 1}{2}, \\ G_{(2,2),(2,2)}|_{\text{tree}} &= \frac{N^4 - 1}{2}, \\ G_{(4),(2,2)}|_{\text{tree}} &= \frac{(N^2 - 1)(2N^2 - 3)}{2N}, \\ G_{(4),(4)}|_{\text{tree}} &= \frac{(N^2 - 1)(N^4 - 6N^2 + 18)}{4N^2}. \end{aligned} \quad (2.11)$$

Explicit expressions can be easily found also for operators with higher dimension.

2.2 One-loop diagrams

We first observe that in the $\mathcal{N} = 4$ theory there are no one-loop corrections to the propagators of the adjoint scalars Φ_I ($I = 1, 2, 3$). At one loop, this is schematically represented in Fig. 2.

$$\frac{a}{I} \longrightarrow \text{wavy loop} \longrightarrow \frac{b}{I} + \frac{a}{I} \longrightarrow \text{circular loop} \longrightarrow \frac{b}{I} = 0$$

Figure 2. The vanishing of the one-loop propagators of the three adjoint scalars Φ_I in the $\mathcal{N} = 4$ theory. The wavy line corresponds to the vector superfield. In the second diagram, the three-point vertices are proportional to the totally anti-symmetric tensor ϵ_{IJK} .

This implies that there is no one-loop correction to the propagator of the adjoint hypermultiplet H in the difference theory.

to Fig. 1(b) is

$$G_{\vec{n},\vec{m}}|_{1\text{-loop}} = n v_{2,1} G_{\vec{n},\vec{m}}|_{\text{tree}} . \quad (2.14)$$

2.3 Two-loop diagrams

At order g_0^4 there are several diagrams that contribute to the correlator (2.6). They are schematically represented by the last four diagrams, from (c) to (f), of Fig. 1. A detailed derivation of the various contributions and the evaluation of the corresponding loop integrals can be found in Appendix B. Here we simply summarize the results for the building blocks of each of these diagrams.

2.3.1 $v_{2,1}^2$ - contributions

The two-loop reducible contributions proportional to $v_{2,1}^2$ arise from two insertions of the one-loop effective interaction vertex (2.12). These can occur either on two different scalar propagators connecting the operators $O_{\vec{n}}$ and $\bar{O}_{\vec{m}}$, or on a single propagator. These two possibilities correspond, respectively, to the diagrams (c) and (d) of Fig. 1.

In the difference theory, the diagram (c) contains as building blocks the diagrams represented in the left-hand side of Fig. 5.

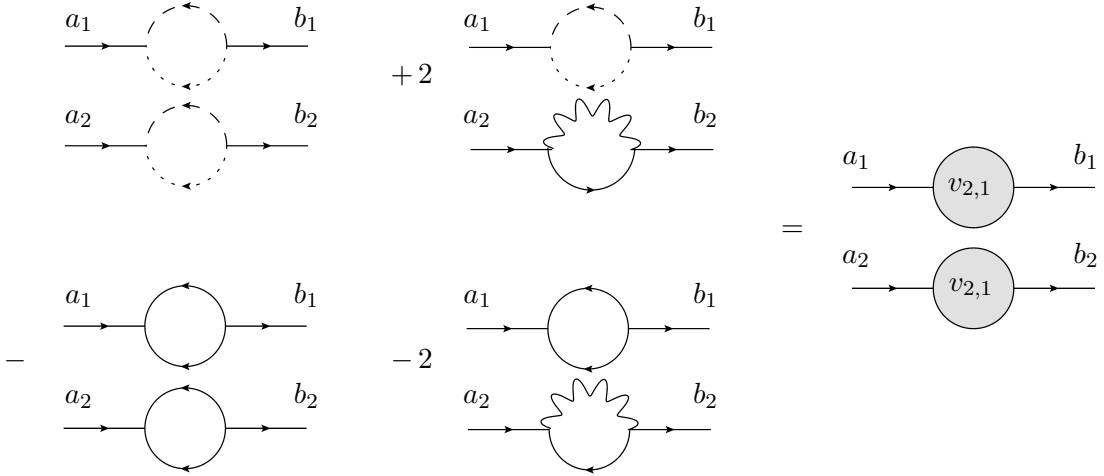


Figure 5. The simultaneous corrections to two scalar propagators in the difference theory can be expressed in terms of the one-loop correction. The factor of 2 in front of the diagrams with the vector field propagator is a multiplicity factor.

If we exploit the identity of Fig. 2 to replace the diagrams with the vector field propagator in favor of the ones with a scalar loop, we can easily realize that the diagrams in the left-hand side Fig. 5 precisely reconstruct the square represented in the right-hand side. Using (2.12), and taking into account the appropriate multiplicity factor of the diagrams, this

gives

$$\begin{array}{c}
a_1 \longrightarrow \text{---} \bigcirc v_{2,1} \text{---} b_1 \\
a_2 \longrightarrow \text{---} \bigcirc v_{2,1} \text{---} b_2
\end{array}
= \frac{1}{2} v_{2,1}^2 \Delta^2(x) \delta^{a_1 b_1} \delta^{a_2 b_2} . \quad (2.15)$$

Let us now consider the contribution corresponding to the two-loop diagram in Fig. 1(d). In this case, the insertion of two one-loop corrections on the same scalar propagator leads to the diagrams displayed in the first two lines of Fig. 6.

$$\begin{aligned}
& + 2 \quad \text{[Diagram: } a \text{ enters a dashed circle, then a dashed circle with a star, then } b \text{]} \\
& - \quad \text{[Diagram: } a \text{ enters a solid circle, then a solid circle with a star, then } b \text{]} \\
& = \quad \text{[Diagram: } a \text{ enters a shaded circle labeled } v_{2,1}, \text{ then another shaded circle labeled } v_{2,1}, \text{ then } b \text{]}
\end{aligned}$$

Figure 6. In the difference theory, the reducible diagrams that correct the φ propagator at two loops can be expressed in terms of the one-loop contribution.

If we use again the identity of Fig. 2 to replace the diagrams containing the vector field propagator with those with a scalar loop, we reconstruct the square of the one-loop correction, as shown in the last line of Fig. 6. Evaluating explicitly the loop integrals in this case, we obtain that the result can be written as the square of the one-loop up to terms of order ϵ (see Appendix B for details), namely

$$a \rightarrow v_{2,1} \rightarrow v_{2,1} \rightarrow b \approx v_{2,1}^2 \Delta(x) \delta^{ab} . \quad (2.16)$$

Here and in the following, we use the approximate symbol \approx for equations that hold up to terms vanishing in the limit $\epsilon \rightarrow 0$.

2.3.2 $v_{2,2}$ - and $v_{4,2}$ - contributions

Let us now consider the two-loop irreducible corrections to the scalar propagator which appear in Fig. 1(e). A first class of contributions arises from correcting one of the internal

lines in the one-loop diagrams of Fig. 4 by using the one-loop propagator of the matter superfields Q and \tilde{Q} , or of the adjoint hypermultiplet H . However, as we have seen before, these contributions vanish.

Other terms that correct the scalar propagator at two loops in the difference theory are those represented in Fig. 7.

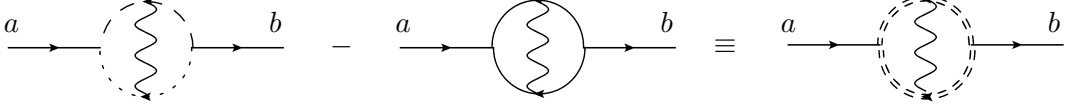


Figure 7. A class of diagrams that correct the scalar propagator at two loops. The dashed double-line notation in the right-hand side is a convenient way to represent this contribution in the difference theory.

Here we have introduced the dashed double-line notation as a convenient way to represent the difference between the loop with fundamental flavors and the loop with the adjoint hypermultiplet. Actually there are other three classes of irreducible diagrams that correct the scalar propagator at two loops. In Fig. 8 we have drawn all such diagrams, whose evaluation is presented in Appendix B to which we refer for details.

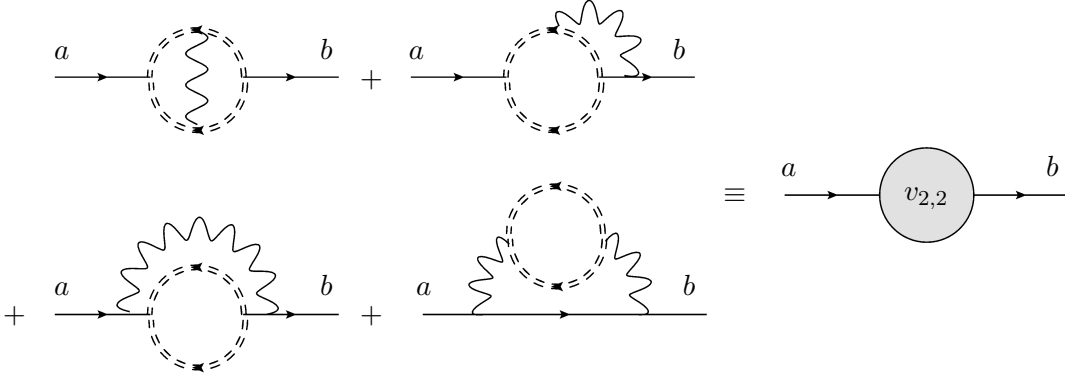


Figure 8. Irreducible two-loop diagrams that correct the φ propagator in the difference theory.

Summing all contributions, we find that the irreducible two-loop correction to the scalar propagator is

$$a \rightarrow \text{shaded circle } v_{2,2} \rightarrow b \equiv v_{2,2} \Delta(x) \delta^{ab}, \quad (2.17)$$

where

$$v_{2,2} \approx -\left(\frac{g_0^2}{8\pi^2}\right)^2 \left[3\zeta(3) \left(\frac{N_f}{2N} + N^2\right) - N(2N - N_f) \frac{\Gamma^2(1 - \epsilon)}{4\epsilon^2(1 - 2\epsilon)(1 + \epsilon)} \right] (\pi x^2)^{2\epsilon}. \quad (2.18)$$

In the difference theory, there are irreducible two-loop contributions that involve two chiral and two anti-chiral fields and give rise to the diagram of Fig. 1(f). These contri-

butions can be further distinguished according to their overall color structure and can be split into two terms which we denote as $v_{4,2}^{(A)}$ and $v_{4,2}^{(B)}$.

The diagrams yielding $v_{4,2}^{(A)}$ are drawn in Fig. 9, where again we have used the dashed double-line notation to represent the difference between Q and H loops.

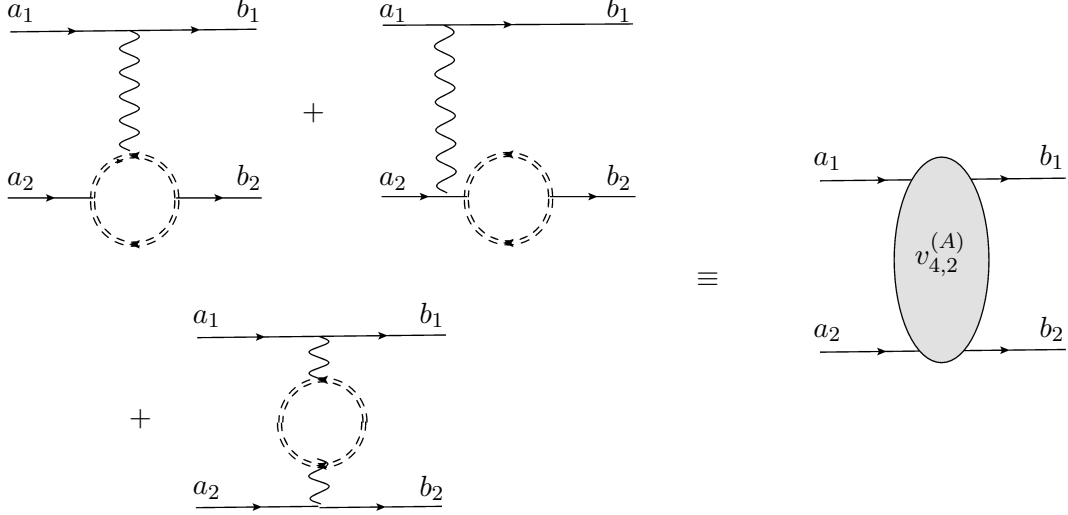


Figure 9. Irreducible two-loop diagrams in the difference theory that yield the $v_{4,2}^{(A)}$ contribution.

They are explicitly evaluated in Appendix B, and the final result is

$$\begin{aligned}
 & \text{Diagram: Ellipse labeled } v_{4,2}^{(A)} \text{ with external lines } a_1, b_1, a_2, b_2 \\
 & \equiv v_{4,2}^{(A)} \Delta^2(x) C_4^{(A) a_1 a_2 b_1 b_2} + \dots, \quad (2.19)
 \end{aligned}$$

where

$$v_{4,2}^{(A)} \approx \left(\frac{g_0^2}{8\pi^2} \right)^2 N (2N - N_f) \left[\frac{21}{2} \zeta(3) + \frac{\Gamma^2(1 - \epsilon)}{4\epsilon^2(1 - 2\epsilon)(1 + \epsilon)} \right] (\pi x^2)^{2\epsilon}, \quad (2.20)$$

$$C_4^{(A) a_1 a_2 b_1 b_2} = -\frac{1}{N} f^{c a_1 b_1} f^{c a_2 b_2}, \quad (2.21)$$

with f^{abc} being the $SU(N)$ structure constants. In (2.19) the ellipses stand for terms with color tensors that are anti-symmetric in (a_1, a_2) and (b_1, b_2) . Such terms do not contribute to the two-point correlation functions (2.5) because they are contracted with the symmetric tensors $R_{\vec{n}}$ and $\bar{R}_{\vec{m}}$ defined in (2.4).

The last two-loop diagram we have to consider is the one represented in Fig. 10.

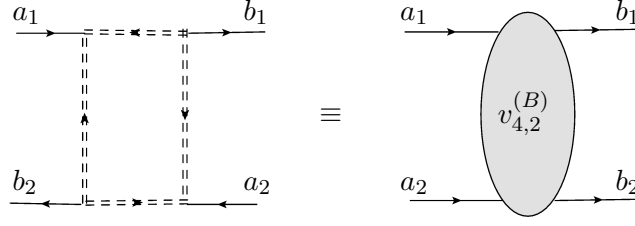


Figure 10. The irreducible two-loop diagram in the difference theory proportional to the colour tensor $C_4^{(B) a_1 a_2 b_1 b_2}$ defined in (2.24).

This diagram was already computed in [15] and the result, which is also reviewed in Appendix B, is

$$\begin{array}{c} a_1 \rightarrow \text{---} \text{---} \text{---} \text{---} \rightarrow b_1 \\ \text{---} \text{---} \text{---} \text{---} \leftarrow \text{---} \text{---} \text{---} \leftarrow a_2 \\ a_2 \rightarrow \text{---} \text{---} \text{---} \text{---} \rightarrow b_2 \end{array} \equiv v_{4,2}^{(B)} \Delta^2(x) C_4^{(B) a_1 a_2 b_1 b_2} + \dots, \quad (2.22)$$

where

$$v_{4,2}^{(B)} \approx \left(\frac{g_0^2}{8\pi^2} \right)^2 3 \zeta(3) (\pi x^2)^{2\epsilon}, \quad (2.23)$$

$$\begin{aligned} C_4^{(B) a_1 a_2 b_1 b_2} &= -(2N - N_f) \text{tr} T^{a_1} T^{b_1} T^{a_2} T^{b_2} \\ &\quad - \frac{1}{2} (\delta^{a_1 b_1} \delta^{a_2 b_2} + \delta^{a_1 a_2} \delta^{b_1 b_2} + \delta^{a_1 b_2} \delta^{a_2 b_1}). \end{aligned} \quad (2.24)$$

Again, the ellipses in (2.22) stand for terms with color tensors which are anti-symmetric in (a_1, a_2) and (b_1, b_2) and, therefore, vanish when inserted in the two-point correlation function.

2.4 Effective vertices

In order to later compare the results of perturbation theory to those of the matrix model, we find it convenient to introduce effective vertices following the ideas of [15]. In particular, to obtain the color dependence of the two-point function $G_{\vec{n}, \vec{m}}$ we strip the x -dependence of the scalar fields and introduce the adjoint matrix $\varphi = \varphi^a T^a$ and its conjugate $\bar{\varphi} = \bar{\varphi}^a T^a$, such that

$$\langle \varphi^a \bar{\varphi}^b \rangle = \delta^{ab}, \quad \langle \varphi^a \varphi^b \rangle = \langle \bar{\varphi}^a \bar{\varphi}^b \rangle = 0. \quad (2.25)$$

We denote by $O_{\vec{n}}(\varphi)$ the operator obtained by replacing in (2.1) the field $\varphi(x)$ with the constant matrix φ , and by $\bar{O}_{\vec{m}}(\bar{\varphi})$ the same with $\bar{\varphi}(x)$ replaced with $\bar{\varphi}$.

With these definitions, it is straightforward to see that the tree-level correlator (2.10) can be written as

$$G_{\vec{n}, \vec{m}}|_{\text{tree}} = \langle O_{\vec{n}}(\varphi) \bar{O}_{\vec{m}}(\bar{\varphi}) \rangle. \quad (2.26)$$

Also the one-loop correlator (2.14) can be written in a simple way using this formalism. Indeed, we have

$$G_{\vec{n},\vec{m}}|_{1\text{-loop}} = v_{2,1} \langle V_2(\varphi, \bar{\varphi}) O_{\vec{n}}(\varphi) \bar{O}_{\vec{m}}(\bar{\varphi}) \rangle , \quad (2.27)$$

where

$$V_2(\varphi, \bar{\varphi}) = \delta^{ab} : \varphi^a \bar{\varphi}^b : = 2 : \text{tr } \varphi \bar{\varphi} : . \quad (2.28)$$

As usual, the notation $: :$ stands for normal ordering. Using (2.25), it is easy to check that inside a vacuum expectation value (2.27) we can use the relation

$$V_2(\varphi, \bar{\varphi}) O_{\vec{n}}(\varphi) = n O_{\vec{n}}(\varphi) \quad (2.29)$$

that follows from the $\text{SU}(N)$ fusion/fission rules

$$\begin{aligned} \text{tr } T^a B_1 T^a B_2 &= \frac{1}{2} \text{tr } B_1 \text{tr } B_2 - \frac{1}{2N} \text{tr } B_1 B_2 , \\ \text{tr } T^a B_1 \text{tr } T^a B_2 &= \frac{1}{2} \text{tr } B_1 B_2 - \frac{1}{2N} \text{tr } B_1 \text{tr } B_2 , \end{aligned} \quad (2.30)$$

valid for two arbitrary $N \times N$ matrices B_1 and B_2 .

Let us now compute the two-loop contribution to the two-point correlation function from diagrams shown in Fig. 1. Using the reducible term (2.15) we find that the contribution of the diagram in Fig. 1(c) is

$$G_{\vec{n},\vec{m}}^{(c)} = \frac{1}{2} n(n-1) v_{2,1}^2 G_{\vec{n},\vec{m}}|_{\text{tree}} . \quad (2.31)$$

In terms of the effective vertex (2.28), this result can be rewritten as follows:

$$\begin{aligned} G_{\vec{n},\vec{m}}^{(c)} &= \frac{1}{2} v_{2,1}^2 \langle : [V_2(\varphi, \bar{\varphi})]^2 : O_{\vec{n}}(\varphi) \bar{O}_{\vec{m}}(\bar{\varphi}) \rangle \\ &= \frac{1}{2} v_{2,1}^2 \left[\langle [V_2(\varphi, \bar{\varphi})]^2 O_{\vec{n}}(\varphi) \bar{O}_{\vec{m}}(\bar{\varphi}) \rangle - 2 \langle V_2(\varphi, \bar{\varphi}) O_{\vec{n}}(\varphi) \bar{O}_{\vec{m}}(\bar{\varphi}) \rangle \right. \\ &\quad \left. - \langle [V_2(\varphi, \bar{\varphi})]^2 \rangle \langle O_{\vec{n}}(\varphi) \bar{O}_{\vec{m}}(\bar{\varphi}) \rangle \right] , \end{aligned} \quad (2.32)$$

where in the second line we have used the identity

$$: V_2(\varphi, \bar{\varphi}) V_2(\varphi, \bar{\varphi}) : = [V_2(\varphi, \bar{\varphi})]^2 - 2 V_2(\varphi, \bar{\varphi}) - \langle [V_2(\varphi, \bar{\varphi})]^2 \rangle \quad (2.33)$$

that follows from Wick's theorem.

The two-loop reducible correction (2.16) to the scalar propagator can be inserted in any of the n internal lines. Thus, the contribution of the diagram in Fig. 1(d) is

$$G_{\vec{n},\vec{m}}^{(d)} \approx n v_{2,1}^2 G_{\vec{n},\vec{m}}|_{\text{tree}} = v_{2,1}^2 \langle V_2(\varphi, \bar{\varphi}) O_{\vec{n}}(\varphi) \bar{O}_{\vec{m}}(\bar{\varphi}) \rangle , \quad (2.34)$$

where we used (2.29). In a similar way, the irreducible two-loop correction (2.17) produces the following contribution to the diagram in Fig. 1(e):

$$G_{\vec{n},\vec{m}}^{(e)} = n v_{2,2} G_{\vec{n},\vec{m}}|_{\text{tree}} = v_{2,2} \langle V_2(\varphi, \bar{\varphi}) O_{\vec{n}}(\varphi) \bar{O}_{\vec{m}}(\bar{\varphi}) \rangle . \quad (2.35)$$

Let us now consider the two-loop contributions proportional to $v_{4,2}^{(A)}$ and $v_{4,2}^{(B)}$ given, respectively, in (2.19) and (2.22). To write the results in a compact form, it is convenient to introduce the quartic vertices

$$\begin{aligned} V_4^{(A)}(\varphi, \bar{\varphi}) &= C_4^{(A) a_1 a_2 b_1 b_2} : \varphi^{a_1} \varphi^{a_2} \bar{\varphi}^{b_1} \bar{\varphi}^{b_2} : \\ &= \frac{2}{N} : \text{tr} [\varphi, \bar{\varphi}]^2 : = \frac{4}{N} (: \text{tr} \varphi \bar{\varphi} \varphi \bar{\varphi} : - : \text{tr} \varphi^2 \bar{\varphi}^2 :) , \end{aligned} \quad (2.36)$$

$$\begin{aligned} V_4^{(B)}(\varphi, \bar{\varphi}) &= C_4^{(B) a_1 a_2 b_1 b_2} : \varphi^{a_1} \varphi^{a_2} \bar{\varphi}^{b_1} \bar{\varphi}^{b_2} : \\ &= -(2N - N_f) : \text{tr} \varphi \bar{\varphi} \varphi \bar{\varphi} : - 4 : (\text{tr} \varphi \bar{\varphi})^2 : - 2 : \text{tr} \varphi \varphi \text{tr} \bar{\varphi} \bar{\varphi} : , \end{aligned} \quad (2.37)$$

Then, the contribution of the effective vertex (2.19) to the correlator can be written as

$$G_{\vec{n}, \vec{m}}^{(A)} = v_{4,2}^{(A)} \langle V_4^{(A)}(\varphi, \bar{\varphi}) O_{\vec{n}}(\varphi) \bar{O}_{\vec{m}}(\bar{\varphi}) \rangle . \quad (2.38)$$

Repeatedly using the fission/fusion identities (2.30), it is possible to show that, inside the vacuum expectation value (2.38), the following relation holds:

$$V_4^{(A)}(\varphi, \bar{\varphi}) \text{tr} \varphi^n = \frac{n}{N} \sum_{\ell=0}^{n-2} (\text{tr} \varphi^{\ell+1} \text{tr} \varphi^{n-\ell-1} - \text{tr} \varphi^\ell \text{tr} \varphi^{n-\ell}) = -n \text{tr} \varphi^n . \quad (2.39)$$

More generally, one can prove that

$$V_4^{(A)}(\varphi, \bar{\varphi}) O_{\vec{n}}(\varphi) = -n O_{\vec{n}}(\varphi) . \quad (2.40)$$

By comparing with (2.29) we conclude that the quartic vertex $V_4^{(A)}$ can be effectively replaced by $(-V_2)$ inside a vacuum expectation value, so that (2.38) becomes

$$G_{\vec{n}, \vec{m}}^{(A)} = -v_{4,2}^{(A)} \langle V_2(\varphi, \bar{\varphi}) O_{\vec{n}}(\varphi) \bar{O}_{\vec{m}}(\bar{\varphi}) \rangle = -n v_{4,2}^{(A)} G_{\vec{n}, \vec{m}}|_{\text{tree}} . \quad (2.41)$$

The contribution of the effective vertex (2.22) to the correlator can be treated in an analogous way, and it reads

$$G_{\vec{n}, \vec{m}}^{(B)} = v_{4,2}^{(B)} \langle V_4^{(B)}(\varphi, \bar{\varphi}) O_{\vec{n}}(\varphi) \bar{O}_{\vec{m}}(\bar{\varphi}) \rangle . \quad (2.42)$$

Notice that, in distinction to the other two-loop contributions, the expectation value (2.42) is not proportional, in general, to the tree-level correlator $G_{\vec{n}, \vec{m}}|_{\text{tree}}$ due to the structure of the vertex $V_4^{(B)}$, and it has to be computed case by case. A few explicit examples with operators of even dimensions are:

$$\begin{aligned} \langle V_4^{(B)}(\varphi, \bar{\varphi}) O_{(2)}(\varphi) \bar{O}_{(2)}(\bar{\varphi}) \rangle &= -\frac{N^2 - 1}{2} \left(N^2 + \frac{N_f}{2N} \right) , \\ \langle V_4^{(B)}(\varphi, \bar{\varphi}) O_{(2,2)}(\varphi) \bar{O}_{(2,2)}(\bar{\varphi}) \rangle &= -\frac{N^2 - 1}{2} \left(2N^4 + 22N^2 - 3NN_f + \frac{7N_f}{N} \right) , \\ \langle V_4^{(B)}(\varphi, \bar{\varphi}) O_{(4)}(\varphi) \bar{O}_{(2,2)}(\bar{\varphi}) \rangle &= -\frac{N^2 - 1}{2} \left(6N^3 - N^2 N_f + 6N + 8N_f - \frac{21N_f}{N^2} \right) , \\ \langle V_4^{(B)}(\varphi, \bar{\varphi}) O_{(4)}(\varphi) \bar{O}_{(4)}(\bar{\varphi}) \rangle &= -\frac{N^2 - 1}{2} \left(12N^2 + NN_f - 18 - \frac{21N_f}{N} + \frac{63N_f}{N^3} \right) . \end{aligned} \quad (2.43)$$

The contribution to the two-point correlator from the two-loop diagram of Fig. 1(f) is given by the sum of (2.41) and (2.42), namely

$$G_{\vec{n},\vec{m}}^{(f)} = -n v_{4,2}^{(A)} G_{\vec{n},\vec{m}}|_{\text{tree}} + v_{4,2}^{(B)} \langle V_4^{(B)}(\varphi, \bar{\varphi}) O_{\vec{n}}(\varphi) \bar{O}_{\vec{m}}(\bar{\varphi}) \rangle, \quad (2.44)$$

where $v_{4,2}^{(A)}$ and $v_{4,2}^{(B)}$ are defined in (2.20) and (2.23), respectively,

2.5 Summary of results

Collecting our findings, up to two loops the bare correlator is given by

$$G_{\vec{n},\vec{m}} \approx \left[1 + n v_{2,1} + \frac{n(n+1)}{2} v_{2,1}^2 \right] G_{\vec{n},\vec{m}}|_{\text{tree}} + n (v_{2,2} - v_{4,2}^{(A)}) G_{\vec{n},\vec{m}}|_{\text{tree}} + v_{4,2}^{(B)} \langle V_4^{(B)}(\varphi, \bar{\varphi}) O_{\vec{n}}(\varphi) \bar{O}_{\vec{m}}(\bar{\varphi}) \rangle. \quad (2.45)$$

The first line contains the tree-level term, the one-loop correction and the reducible two-loop part, while the irreducible two-loop terms are written in the second line.

Eq. (2.45) is the main result of this section. It expresses the bare two-point correlator between chiral and anti-chiral operators up to order g_0^4 , in terms of the tree-level correlator and the matrix model correlator with the insertion of the quartic effective vertex $V_4^{(B)}$. Moreover, it exhibits a particularly simple structure of the UV divergences of $G_{\vec{n},\vec{m}}$. First, we notice that all divergent terms in the difference $(v_{2,2} - v_{4,2}^{(A)})$ exactly cancel. Indeed, using (2.18) and (2.20), we have

$$v_{2,2} - v_{4,2}^{(A)} \approx -3\zeta(3) \left(\frac{g_0^2}{8\pi^2} \right)^2 \left(8N^2 - \frac{7NN_f}{2} + \frac{N_f}{2N} \right). \quad (2.46)$$

This, together with the fact that

$$v_{4,2}^{(B)} \approx 3\zeta(3) \left(\frac{g_0^2}{8\pi^2} \right)^2, \quad (2.47)$$

implies that the total two-loop irreducible contribution in the second line of (2.45) is finite for $\epsilon \rightarrow 0$. The only divergences remaining at two loops come from the square of those present at one-loop. At the given loop order, they can be nicely combined into an overall factor (see the first line of (2.45))

$$1 + n v_{2,1} + \frac{n(n+1)}{2} v_{2,1}^2 + \dots = \frac{1}{(1 - v_{2,1})^n}, \quad (2.48)$$

which depends only on the bare dimension n of the operators but not on their detailed structure.

We conclude this section by showing that the two-loop result (2.45) can be rewritten in an alternative and elegant form as a correlator in the matrix model. Combining the tree-level, one-loop and two-loop contributions given in (2.26), (2.27), (2.32), (2.34), (2.35) and (2.44), we obtain

$$G_{\vec{n},\vec{m}} \approx \langle O_{\vec{n}}(\varphi) \bar{O}_{\vec{m}}(\bar{\varphi}) \rangle + (v_{2,1} + v_{2,2} - v_{4,2}^{(A)}) \langle V_2(\varphi, \bar{\varphi}) O_{\vec{n}}(\varphi) \bar{O}_{\vec{m}}(\bar{\varphi}) \rangle + \frac{1}{2} v_{2,1}^2 \left[\langle [V_2(\varphi, \bar{\varphi})]^2 O_{\vec{n}}(\varphi) \bar{O}_{\vec{m}}(\bar{\varphi}) \rangle - \langle [V_2(\varphi, \bar{\varphi})]^2 \rangle \langle O_{\vec{n}}(\varphi) \bar{O}_{\vec{m}}(\bar{\varphi}) \rangle \right] + v_{4,2}^{(B)} \langle V_4^{(B)}(\varphi, \bar{\varphi}) O_{\vec{n}}(\varphi) \bar{O}_{\vec{m}}(\bar{\varphi}) \rangle. \quad (2.49)$$

Then, defining the effective interaction vertex

$$V_{\text{eff}}(\varphi, \bar{\varphi}) = -(v_{2,1} + v_{2,2} - v_{4,2}^{(A)}) V_2(\varphi, \bar{\varphi}) - v_{4,2}^{(B)} V_4^{(B)}(\varphi, \bar{\varphi}) , \quad (2.50)$$

we can recast (2.49) in a very compact way as follows:

$$G_{\vec{n}, \vec{m}} \approx \frac{\langle e^{-V_{\text{eff}}(\varphi, \bar{\varphi})} O_{\vec{n}}(\varphi) \bar{O}_{\vec{m}}(\bar{\varphi}) \rangle}{\langle e^{-V_{\text{eff}}(\varphi, \bar{\varphi})} \rangle} . \quad (2.51)$$

Indeed, expanding the exponentials up to order g_0^4 , we precisely recover all terms of (2.49). In particular, from the insertion of a single V_{eff} in the correlator we obtain the linear terms in the $v_{k\ell}$'s appearing in the first and third line of (2.49), while the quadratic terms in the second line arise from two insertions of V_{eff} . Notice that since this effective vertex is normal-ordered, the denominator in (2.51) contributes up to order g_0^4 only with the term proportional to $\langle [V_2(\varphi, \bar{\varphi})]^2 \rangle$ appearing in the second line of (2.49).

In Section 4 we show that localization on a four sphere produces an expression similar to (2.51). However, in order to compare the two expressions, we should first get rid of the UV divergences and scheme ambiguities that are present in the bare correlator $G_{\vec{n}, \vec{m}}$. This is the content of the next section.

3 Renormalization

The dimensionally regularized bare correlators $G_{\vec{n}, \vec{m}}$ given in (2.45) are divergent for $\epsilon \rightarrow 0$, since the one-loop coefficient $v_{2,1}$ defined in (2.13) behaves for small ϵ as

$$v_{2,1} \approx \frac{g_0^2}{16\pi^2} (\pi x^2)^\epsilon (2N - N_f) \left(\frac{1}{\epsilon} + 2 + \gamma_E \right) . \quad (3.1)$$

As we have remarked before, the UV divergence due to $v_{2,1}$ is the only one that plagues the correlators, since all other terms in $G_{\vec{n}, \vec{m}}$ are finite for $\epsilon \rightarrow 0$. To get rid of this divergence, we have to apply the standard renormalization procedure. First, we introduce the dimensionless renormalized gauge coupling constant g through the relation

$$g_0^2 = \mu^{2\epsilon} g^2 Z(g^2, \epsilon) , \quad (3.2)$$

where μ is an arbitrary scale, and Z is a suitable function to be determined. Then, we define the renormalized operators $O_{\vec{n}}^R(x)$ according to

$$O_{\vec{n}}^R(x) = \sum_{\vec{m}} Z_{\vec{n}}^{\vec{m}}(g^2, \epsilon) O_{\vec{m}}(x) , \quad (3.3)$$

where $Z_{\vec{n}}^{\vec{m}}$ is a matrix-valued function. However, in the previous section we have shown that the divergences of the two-point functions depend only on the scaling dimensions of the operators and not on the operator details; therefore a block-diagonal matrix can do the job, and we can simplify (3.3) by setting

$$O_{\vec{n}}^R(x) = Z_n(g^2, \epsilon) O_{\vec{n}}(x) . \quad (3.4)$$

A similar formula holds for the anti-chiral renormalized operators $\bar{O}_{\vec{n}}^R(x)$.

The singular terms of the functions $Z(g^2, \epsilon)$ and $Z_n(g^2, \epsilon)$ are determined by requiring that the correlator $\langle O_{\vec{n}}^R(x) \bar{O}_{\vec{m}}^R(0) \rangle$ should be finite when expressed in terms of the renormalized coupling g . This means that the renormalized correlator

$$G_{\vec{n}, \vec{m}}^R = Z_n^2(g^2, \epsilon) G_{\vec{n}, \vec{m}} \Big|_{g_0^2 = \mu^{2\epsilon} g^2 Z(g^2, \epsilon)} \quad (3.5)$$

is well-defined and free of divergences in the limit $\epsilon \rightarrow 0$.

3.1 The β -function and anomalous dimensions

The dependence of the renormalized coupling g^2 and of the renormalization constant $Z_n(g^2, \epsilon)$ on the energy scale μ is described, respectively, by the β -function and by the anomalous dimensions $\gamma_n(g^2)$ of the operators $O_{\vec{n}}$. They are defined as follows:

$$\beta(g^2) \equiv \mu \frac{dg^2}{d\mu} = -2\epsilon g^2 - g^2 \mu \frac{d \ln Z(g^2, \epsilon)}{d\mu}, \quad (3.6)$$

where the last equality stems from the μ -independence of g_0 , and

$$\gamma_n(g^2) \equiv -\mu \frac{d \ln Z_n(g^2, \epsilon)}{d\mu} = -\beta(g^2) \frac{d \ln Z_n(g^2, \epsilon)}{dg^2}, \quad (3.7)$$

where in the second step we used (3.6). Using the perturbative expansions

$$\begin{aligned} \beta(g^2) &= -2\epsilon g^2 + \beta_0 g^4 + \beta_1 g^6 + \dots, \\ \gamma_n(g^2) &= \gamma_{n,0} g^2 + \gamma_{n,1} g^4 + \dots, \end{aligned} \quad (3.8)$$

we can explicitly integrate (3.6) and (3.7) and get in the minimal subtraction (MS) scheme

$$\begin{aligned} Z(g^2, \epsilon) &= \exp \left[- \int_0^{g^2} dt \frac{\beta(t) + 2\epsilon t}{\beta(t)} \right] = 1 + g^2 \frac{\beta_0}{2\epsilon} + g^4 \left(\frac{\beta_0^2}{4\epsilon^2} + \frac{\beta_1}{4\epsilon} \right) + \dots, \\ Z_n(g^2, \epsilon) &= \exp \left[- \int_0^{g^2} dt \frac{\gamma_n(t)}{\beta(t)} \right] = 1 + g^2 \frac{\gamma_{n,0}}{2\epsilon} + g^4 \left(\frac{\beta_0 \gamma_{n,0} + \gamma_{n,0}^2}{8\epsilon^2} + \frac{\gamma_{n,1}}{4\epsilon} \right) + \dots. \end{aligned} \quad (3.9)$$

This shows that the expansion coefficients of the β -function and of the anomalous dimensions γ_n are directly related to the coefficients of the $1/\epsilon$ -terms in Z and Z_n respectively.

Differentiating (3.5) and using $dG_{\vec{n}, \vec{m}}/d\mu = 0$, one obtains the Callan-Symanzik equation

$$\left(\mu \frac{\partial}{\partial \mu} + \beta(g^2) \frac{\partial}{\partial g^2} + 2\gamma_n(g^2) \right) G_{\vec{n}, \vec{m}}^R = 0 \quad (3.10)$$

on which we can safely take the limit $\epsilon \rightarrow 0$.

We now determine the coefficients of the β -function and the anomalous dimensions, using the explicit results of the previous section. To do so, we expand the bare correlator (2.45) for small ϵ using (3.1), and write

$$G_{\vec{n}, \vec{m}} = \alpha_0 + g_0^2 \left(\frac{\alpha_{1,1}}{\epsilon} + \alpha_{1,0} + \dots \right) + g_0^4 \left(\frac{\alpha_{2,2}}{\epsilon^2} + \frac{\alpha_{2,1}}{\epsilon} + \dots \right) + O(g_0^6), \quad (3.11)$$

where $\alpha_0 = G_{\vec{n}, \vec{m}}|_{\text{tree}}$ and

$$\begin{aligned}\alpha_{1,1} &= n \frac{2N - N_f}{16\pi^2} \alpha_0, & \alpha_{1,0} &= n \frac{(2N - N_f)(2 + \gamma_E + \ln \pi x^2)}{16\pi^2} \alpha_0, \\ \alpha_{2,2} &= n(n+1) \frac{(2N - N_f)^2}{512\pi^4} \alpha_0, & \alpha_{2,1} &= n(n+1) \frac{(2N - N_f)^2(2 + \gamma_E + \ln \pi x^2)}{256\pi^4} \alpha_0.\end{aligned}\quad (3.12)$$

Plugging the expansion (3.11) into the renormalized correlator (3.5), using (3.9) and requiring that all divergent terms cancel, one finds

$$\beta_0 = \frac{2(\alpha_{1,1}^2 - 2\alpha_0\alpha_{2,2})}{\alpha_0\alpha_{1,1}}, \quad \gamma_{n,0} = -\frac{\alpha_{1,1}}{\alpha_0}, \quad \gamma_{n,1} = \frac{2(2\alpha_{1,0}\alpha_{2,2} - \alpha_{1,1}\alpha_{2,1})}{\alpha_0\alpha_{1,1}}, \quad (3.13)$$

leading to

$$\beta_0 = -\frac{2N - N_f}{8\pi^2}, \quad \gamma_{n,0} = -n\frac{2N - N_f}{16\pi^2}, \quad \gamma_{n,1} = 0. \quad (3.14)$$

This value of β_0 is in agreement with the well-known result for the one-loop coefficient of the β -function in $\mathcal{N} = 2$ SQCD. We also notice that $\gamma_{2,0} = \beta_0$. This is consistent with $\mathcal{N} = 2$ supersymmetry, since the chiral operator $O_{(2)} = \text{tr} \varphi^2$ and the Yang-Mills Lagrangian $-\text{tr}(F^2/4) + \dots$ belong to the same supermultiplet, and thus should renormalize in the same way, that is

$$Z_2(g^2, \epsilon) = Z(g^2, \epsilon). \quad (3.15)$$

Moreover, using the fact that in $\mathcal{N} = 2$ SYM theories the β -function receives only one-loop correction², *i.e.* $\beta_\ell = 0$ for all $\ell \geq 1$, we conclude that also the anomalous dimensions of $\text{tr} \varphi^2$ are corrected only at one loop, *i.e.* $\gamma_{2,\ell} = 0$ for all $\ell \geq 1$. This implies that

$$Z_2(g^2, \epsilon) = Z(g^2, \epsilon) = 1 - \frac{g^2(2N - N_f)}{16\pi^2 \epsilon} + \frac{g^4(2N - N_f)^2}{256\pi^4 \epsilon^2} + \dots = \frac{1}{1 + \frac{g^2(2N - N_f)}{16\pi^2 \epsilon}}. \quad (3.16)$$

Furthermore, we deduce from (3.14) that the following relation

$$Z_n(g^2, \epsilon) = [Z(g^2, \epsilon)]^{\frac{n}{2}} \quad (3.17)$$

holds up to two loops. It would be very interesting to investigate whether this relation holds also at higher loops. While this issue is not relevant for the two-loop analysis of the present paper, it is tempting to speculate that (3.17) might actually be true in general. Indeed, in our set-up the anomalous dimensions of the chiral and anti-chiral operators arise because of the breaking of conformal invariance at the quantum level due to dimensional transmutation. The fact that the coefficients $\gamma_{n,0}$ and β_0 are proportional to each other and that the proportionality factor is $n/2$ (see (3.14)), together with $\mathcal{N} = 2$ supersymmetry, naturally leads one to propose the relation (3.17). Notice that in the conformal case $N_f = 2N$, the renormalization functions simply reduce to 1, due to the absence of divergences, so that (3.17) is trivially satisfied in this case.

²This fact has been tested by explicit computations at two loops, see for example [19–21], and then extended to all loops using non-renormalization and anomaly arguments, and further strengthened at the non-perturbative level [22–24].

3.2 Renormalized correlators

Using the previous results, it is easy to see that up to two loops and in the limit $\epsilon \rightarrow 0$, the renormalized correlators (3.5) take a form completely analogous to the bare correlators (2.45), namely

$$G_{\vec{n},\vec{m}}^R = \left[1 + n c_1 + \frac{n(n+1)}{2} c_1^2 + n c_2 \right] G_{\vec{n},\vec{m}}|_{\text{tree}} + c_3 \langle V_4^{(B)}(\varphi, \bar{\varphi}) O_{\vec{n}}(\varphi) \bar{O}_{\vec{m}}(\bar{\varphi}) \rangle, \quad (3.18)$$

where

$$\begin{aligned} c_1 &= \frac{g^2}{16\pi^2} \nu (2N - N_f), \\ c_2 &= -3\zeta(3) \left(\frac{g^2}{8\pi^2} \right)^2 \left(8N^2 - \frac{7NN_f}{2} + \frac{N_f}{2N} \right), \\ c_3 &= 3\zeta(3) \left(\frac{g^2}{8\pi^2} \right)^2, \end{aligned} \quad (3.19)$$

and

$$\nu = 2 + \gamma_E + \ln \pi \mu^2 x^2. \quad (3.20)$$

The coefficients c_i are obtained from (3.1), (2.46) and (2.47). In the conformal case c_1 vanishes and the first perturbative correction to the correlator appears at order g^4 .

Performing the same manipulations as described in Section 2 for the bare correlators, we can rewrite (3.18) in the following form:

$$G_{\vec{n},\vec{m}}^R = \frac{\langle e^{-V_{\text{eff}}^R(\varphi, \bar{\varphi})} O_{\vec{n}}(\varphi) \bar{O}_{\vec{m}}(\bar{\varphi}) \rangle}{\langle e^{-V_{\text{eff}}^R(\varphi, \bar{\varphi})} \rangle} + O(g^6), \quad (3.21)$$

$$V_{\text{eff}}^R(\varphi, \bar{\varphi}) = -(c_1 + c_2) V_2(\varphi, \bar{\varphi}) - c_3 V_4^{(B)}(\varphi, \bar{\varphi}), \quad (3.22)$$

where the two- and four-point vertices V_2 and $V_4^{(B)}$ are defined, respectively, in (2.28) and (2.37).

We remark that for $N_f \neq 2N$, the renormalized correlator $G_{\vec{n},\vec{m}}^R$ is *not* a constant, but it depends on x through the $\ln \pi \mu^2 x^2$ term contained in ν . At first sight, this fact makes it unlikely that the correlator can be encoded in a matrix model. However, the dependence of $G_{\vec{n},\vec{m}}^R$ on ν is determined by the Callan-Symanzik equation (3.10)³ and by its value at a reference point $\hat{\nu}$. For instance, setting

$$\mu^2 x^2 = \frac{e^{\gamma_E}}{\pi}, \quad (3.23)$$

³This equation requires that the correlator must have the form

$$G_{\vec{n},\vec{m}}^R = d_0 + g^2(d_1 - d_0 \gamma_{n,0} \nu) + g^4 \left[d_2 - \nu d_0 \gamma_{n,1} + \frac{\nu}{4} (\nu d_0 \gamma_{n,0} - 2d_1)(\beta_0 + 2\gamma_{n,0}) \right] + O(g^6).$$

It is easy to check that (3.18) satisfies this requirement. Notice that the whole ν -dependence of $G_{\vec{n},\vec{m}}^R$ can be reconstructed order by order in g^2 from the correlator at a given value $\hat{\nu}$, for instance $\hat{\nu} = 0$, and the coefficients β_0 , $\gamma_{n,0}$ and $\gamma_{n,1}$.

we get from (3.20)

$$\widehat{\nu} = 2(1 + \gamma_E) , \quad (3.24)$$

which, as we will see in Section 4, is the combination that matches the one-loop matrix model results from localization. In particular, with the choice (3.23) the coefficient c_1 becomes

$$c_1 = \frac{g^2}{8\pi^2} (1 + \gamma_E) (2N - N_f) . \quad (3.25)$$

Using (2.11) and (2.43) we find from (3.18)

$$G_{(2),(2)}^R = \frac{N^2 - 1}{2} \left[1 + 2c_1 + 3c_1^2 + 2c_2 - c_3 \left(N^2 + \frac{N_f}{2N} \right) \right] + O(g^6) . \quad (3.26)$$

Similar explicit formulae can be worked out for correlators involving higher dimensional operators. For example, at dimension 4 we find

$$G_{(2,2),(2,2)}^R = \frac{N^4 - 1}{2} \left(1 + 4c_1 + 10c_1^2 + 4c_2 \right) - c_3 \frac{(N^2 - 1)}{2} \left(2N^4 + 22N^2 - 3NN_f + \frac{7N_f}{N} \right) + O(g^6) , \quad (3.27a)$$

$$G_{(4),(2,2)}^R = \frac{2N^4 - 5N^2 + 3}{2N} \left(1 + 4c_1 + 10c_1^2 + 4c_2 \right) - c_3 \frac{(N^2 - 1)}{2} \left(6N^3 - N^2N_f + 6N + 8N_f - \frac{21N_f}{N^2} \right) + O(g^6) , \quad (3.27b)$$

$$G_{(4),(4)}^R = \frac{N^6 - 7N^4 + 24N^2 - 18}{4N^2} \left(1 + 4c_1 + 10c_1^2 + 4c_2 \right) - c_3 \frac{(N^2 - 1)}{2} \left(12N^2 + NN_f - 18 - \frac{21N_f}{N} + \frac{63N_f}{N^3} \right) + O(g^6) , \quad (3.27c)$$

where the coefficients c_1 , c_2 and c_3 are defined in (3.19). Notice that c_1 and c_2 enter into these expressions in the same combination.

3.3 Normalized correlators

The renormalized correlators $G_{\vec{n},\vec{m}}^R$ are finite but they cannot be considered as physical observables since they depend on the choice of the renormalization scheme. In particular, given a renormalized correlator at a certain normalization scale μ , one can always perform a finite renormalization of the operators by multiplying the renormalization factors Z and Z_n defined in (3.2) and (3.4), respectively, by an arbitrary finite function of the coupling. This transformation preserves the UV finiteness of the correlator and corresponds to a change of the renormalization scheme (see, for example, [25] for a discussion of this point in a different context).

Since, up to two loops we have $Z_n = (Z_2)^{\frac{n}{2}}$, we can eliminate the scheme dependence by considering dimensionless ratios of correlators. In fact, the renormalized correlators can be written as

$$G_{\vec{n},\vec{m}}^R = \frac{1}{(1 - c_1 - c_2)^n} \left[G_{\vec{n},\vec{m}}|_{\text{tree}} + c_3 \langle V_4^{(B)}(\varphi, \bar{\varphi}) O_{\vec{n}}(\varphi) \bar{O}_{\vec{m}}(\bar{\varphi}) \rangle \right] + O(g^6) . \quad (3.28)$$

This relation shows that the dependence on x^2 and on the renormalization scale μ coming from the coefficient c_1 is entirely encoded in a prefactor which only depends on the bare scaling dimension n of the operators but not on their specific form. Therefore, this prefactor cancels in the ratio of correlators of operators of the same dimension. Choosing, for example, as a reference the correlator between two operators $O_{(2)}$, which are the only ones with dimension 2, we are led to introduce the normalized correlators

$$A_{\vec{n},\vec{m}}^R = \frac{G_{\vec{n},\vec{m}}^R}{[G_{(2),(2)}^R]^{\frac{n}{2}}} . \quad (3.29)$$

These ratios are independent of the choice of the renormalization scale μ and scheme, and as such they represent physical quantities.

It is interesting to observe that the two-loop contribution to the ratio $A_{\vec{n},\vec{m}}^R$ only comes from the irreducible diagram represented in Fig. 10, which is finite in the limit $\epsilon \rightarrow 0$ (see (2.22) and (2.23)). This shows that also the bare ratios

$$A_{\vec{n},\vec{m}} = \frac{G_{\vec{n},\vec{m}}}{[G_{(2),(2)}]^{\frac{n}{2}}} = A_{\vec{n},\vec{m}}^R \quad (3.30)$$

are finite. The equality between $A_{\vec{n},\vec{m}}$ and $A_{\vec{n},\vec{m}}^R$ comes from the fact that the Z_n -factors cancel between the numerator and denominators, and the Z -renormalization of the gauge coupling starts to contribute at the next order. One can check this explicitly, by writing the bare correlators (2.45) as

$$G_{\vec{n},\vec{m}} = \frac{1}{(1 - v_{2,1} - v_{2,2} + v_{4,2}^{(A)})^n} \left[G_{\vec{n},\vec{m}}|_{\text{tree}} + v_{4,2}^{(B)} \langle V_4^{(B)}(\varphi, \bar{\varphi}) O_{\vec{n}}(\varphi) \bar{O}_{\vec{m}}(\bar{\varphi}) \rangle \right] + O(g_0^6) , \quad (3.31)$$

which shows that the divergence encoded in the one-loop coefficient $v_{2,1}$ cancels in the ratios $A_{\vec{n},\vec{m}}$. Furthermore, by comparing (3.31) and (3.28), we can realize that the bare and the renormalized ratios match at two loops, apart from the obvious replacement of g_0 with g .

The explicit expressions of the normalized correlators for operators of dimension 4 are:

$$A_{(22),(22)}^R = \frac{2(N^2 + 1)}{N^2 - 1} - \frac{3g^4\zeta(3)}{16\pi^4} \frac{(10N^3 - 2N^2N_f + 3N_f)}{N(N^2 - 1)} , \quad (3.32a)$$

$$A_{(4),(22)}^R = \frac{2(2N^2 - 3)}{N(N^2 - 1)} - \frac{3g^4\zeta(3)}{32\pi^4} \frac{(2N^5 + 12N^3 - N^4N_f + 6N^2N_f - 18N_f)}{N^2(N^2 - 1)} , \quad (3.32b)$$

$$A_{(4),(4)}^R = \frac{N^4 - 6N^2 + 18}{N^2(N^2 - 1)} + \frac{3g^4\zeta(3)}{64\pi^4} \frac{(2N^7 - 36N^5 + 72N^3 - N^4N_f + 36N^2N_f - 108N_f)}{N^3(N^2 - 1)} . \quad (3.32c)$$

Similar formulae can be easily found also for operators of other dimensions.

In the next section we will recover this same result from the matrix model obtained by applying localization on the sphere S^4 .

4 Matrix model approach

In [6] it was shown, using localization techniques, that the partition function of a $\mathcal{N} = 2$ SYM theory with gauge group $SU(N)$ defined on a four-sphere S^4 can be written in terms of a traceless Hermitian $N \times N$ matrix a in the following way:

$$\mathcal{Z}_{S^4} = \int \prod_{u=1}^N da_u \Delta(a) |Z(\mathrm{i}a, \tau)|^2 \delta\left(\sum_{v=1}^N a_v\right). \quad (4.1)$$

Here we have denoted by a_u the (real) eigenvalues of a , by $\Delta(a)$ the Vandermonde determinant

$$\Delta(a) = \prod_{u < v=1}^N a_{uv}^2, \quad (4.2)$$

where $a_{uv} = a_u - a_v$, and for simplicity have set to 1 the radius R of the four-sphere⁴. Furthermore, $Z(\mathrm{i}a, \tau)$ is the gauge theory partition function with τ being the complexified gauge coupling:

$$\tau = \frac{\theta}{2\pi} + \mathrm{i} \frac{4\pi}{g^2}. \quad (4.3)$$

In this paper we actually set the θ -angle to zero. We remark that in the non-conformal theories the coupling g appearing in the matrix model has to be interpreted as the renormalized gauge coupling at a scale proportional to the inverse radius of the four-sphere [6].

The gauge theory partition function $Z(\mathrm{i}a, \tau)$ is computed using the localization techniques of [26, 27] with a purely imaginary vacuum expectation value $\langle \varphi \rangle = \mathrm{i}a$ for the adjoint scalar, and an Ω -background with parameters $\epsilon_1 = \epsilon_2 = 1/R$. This partition function can be written as a product of the classical, one-loop and instanton contributions, namely

$$Z(\mathrm{i}a, \tau) = Z_{\text{class}}(\mathrm{i}a, \tau) Z_{\text{one-loop}}(\mathrm{i}a) Z_{\text{inst}}(\mathrm{i}a, \tau). \quad (4.4)$$

Since we work at weak coupling $g^2 \ll 1$, where instantons are exponentially suppressed, we can set $Z_{\text{inst}}(\mathrm{i}a) = 1$. The classical part produces a simple Gaussian term in the matrix model:

$$|Z_{\text{class}}(\mathrm{i}a, \tau)|^2 = \mathrm{e}^{-\frac{8\pi^2}{g^2} \sum_u a_u^2} = \mathrm{e}^{-\frac{8\pi^2}{g^2} \text{tr } a^2}. \quad (4.5)$$

The one-loop contribution arising from the gauge multiplet and N_f matter multiplets can be written as [6] (see also [15] for details)

$$|Z_{1\text{-loop}}(\mathrm{i}a)|^2 = \mathrm{e}^{-S_2(a) - S_4(a) + \dots} \quad (4.6)$$

⁴The dependence on R can be easily restored by replacing a_u with $a_u R$.

where $S_n(a)$ are homogeneous polynomials in a of order n . The first few of them are:

$$S_2(a) = -(1 + \gamma_E) \left(\sum_{u,v=1}^N a_{uv}^2 - N_f \sum_{u=1}^N a_u^2 \right) = -(1 + \gamma_E) (2N - N_f) \text{tr } a^2, \quad (4.7a)$$

$$S_4(a) = \frac{\zeta(3)}{2} \left(\sum_{u,v=1}^N a_{uv}^4 - N_f \sum_{u=1}^N a_u^4 \right) = \frac{\zeta(3)}{2} \left[(2N - N_f) \text{tr } a^4 + 6 (\text{tr } a^2)^2 \right], \quad (4.7b)$$

$$S_6(a) = -\frac{\zeta(5)}{3} \left(\sum_{u,v=1}^N a_{uv}^6 - N_f \sum_{u=1}^N a_u^6 \right) = -\frac{\zeta(5)}{3} \left[(2N - N_f) \text{tr } a^6 + 30 \text{tr } a^4 \text{tr } a^2 - 20 (\text{tr } a^3)^2 \right]. \quad (4.7c)$$

Performing the rescaling

$$a \rightarrow \left(\frac{g^2}{8\pi^2} \right)^{\frac{1}{2}} a, \quad (4.8)$$

the matrix model gets a canonically normalized Gaussian factor and the sphere partition function (4.1) becomes

$$\mathcal{Z}_{S^4} = \left(\frac{g^2}{8\pi^2} \right)^{\frac{N^2-1}{2}} \int \prod_{u=1}^N da_u \Delta(a) e^{-\text{tr } a^2 - S_{\text{int}}(a)} \delta \left(\sum_{v=1}^N a_v \right) \quad (4.9)$$

with

$$S_{\text{int}}(a) = \frac{g^2}{8\pi^2} S_2(a) + \left(\frac{g^2}{8\pi^2} \right)^2 S_4(a) + \left(\frac{g^2}{8\pi^2} \right)^3 S_6(a) + \dots. \quad (4.10)$$

The term of order $g^{2\ell}$ in $S_{\text{int}}(a)$ accounts for effects that take place at ℓ loops in the corresponding field theory computation. Therefore we will refer to the g^2 -expansion of S_{int} as a loop expansion.

Exploiting the Vandermonde determinant $\Delta(a)$ and writing $a = a^b T^b$, we can alternatively express the integral (4.9) using a flat integration measure da over all matrix components a^b as follows

$$\mathcal{Z}_{S^4} = c_N \left(\frac{g^2}{8\pi^2} \right)^{\frac{N^2-1}{2}} \int da e^{-\text{tr } a^2 - S_{\text{int}}(a)} \quad (4.11)$$

where c_N is a g -independent constant and $da \propto \prod_b da^b$. The overall prefactors in (4.11) are irrelevant when computing correlators and thus can be neglected.

Given any function $f(a)$, its vacuum expectation value in the matrix model described above is defined as follows

$$\begin{aligned} \langle f(a) \rangle &= \frac{1}{\mathcal{Z}_{S^4}} \int \prod_{u=1}^N da_u \Delta(a) |Z(\text{ia}, \tau)|^2 \delta \left(\sum_{v=1}^N a_v \right) f(a) \\ &= \frac{\int da e^{-\text{tr } a^2 - S_{\text{int}}(a)} f(a)}{\int da e^{-\text{tr } a^2 - S_{\text{int}}(a)}} = \frac{\langle e^{-S_{\text{int}}(a)} f(a) \rangle_0}{\langle e^{-S_{\text{int}}(a)} \rangle_0}, \end{aligned} \quad (4.12)$$

where in the second line we have used (4.11). The subscript “0” denotes the vacuum expectation values taken with respect to the Gaussian measure, which can be computed by repeatedly using Wick’s theorem to reduce them to the basic contraction

$$\langle a^b a^c \rangle_0 = \delta^{bc} . \quad (4.13)$$

4.1 Chiral and anti-chiral operators in the matrix model

We are interested in extracting from the matrix model (4.12) the two-point functions (2.5). To this aim we have first to find counter-partners of the chiral and anti-chiral operators in the matrix model. It would seem natural to associate to the multi-trace operator $O_{\vec{n}}(x)$ defined in (2.1), an analogous function $O_{\vec{n}}(a)$ in the matrix model, given by the same expression (2.1) but with $\varphi(x)$ replaced by a , namely

$$O_{\vec{n}}(a) = \text{tr } a^{n_1} \text{tr } a^{n_2} \dots \text{tr } a^{n_\ell} . \quad (4.14)$$

However, the operator $O_{\vec{n}}(x)$ has vanishing vacuum expectation value in the field theory, while in the matrix model $\langle O_{\vec{n}}(a) \rangle \neq 0$ due to the self-contractions of a . This means that we have to refine the dictionary and make $O_{\vec{n}}(a)$ normal-ordered. This can be done by subtracting from $O_{\vec{n}}(a)$ all possible self-contractions and making it orthogonal to all operators with lower dimensions.

As discussed in [15, 16, 28], the prescription to define the normal ordering of any operator $O(a)$ in the matrix model is the following. Let be Δ the dimension of $O(a)$ and $\{O_p(a)\}$ a basis in the finite-dimensional space of matrix operators with dimension smaller than Δ . Denoting by C_Δ the (finite-dimensional) matrix of correlators

$$(C_\Delta)_{pq} = \langle O_p(a) O_q(a) \rangle , \quad (4.15)$$

which are computed according to (4.12), we define the normal-ordered operator as

$$:O(a):_g = O(a) - \sum_{p,q} \langle O(a) O_p(a) \rangle (C_\Delta^{-1})^{pq} O_q(a) . \quad (4.16)$$

Our notation stresses the fact that this normal-ordering is g -dependent, since the correlators on the right hand side of (4.16) are computed in the interacting matrix model. The proposal is then to associate to the field theory operators the corresponding normal-ordered matrix operators, namely

$$O_{\vec{n}}(x) \rightarrow \mathcal{O}_{\vec{n}}(a) = :O_{\vec{n}}(a):_g . \quad (4.17)$$

A similar replacement holds for the anti-chiral operators.

For example, using the definition (4.16) we find

$$\begin{aligned} \mathcal{O}_{(2)}(a) = \text{tr } a^2 - \frac{N^2 - 1}{2} \left[1 + \frac{g^2}{8\pi^2} (1 + \gamma_E)(2N - N_f) + \left(\frac{g^2}{8\pi^2} \right)^2 (1 + \gamma_E)^2 (2N - N_f)^2 \right. \\ \left. - \left(\frac{g^2}{8\pi^2} \right)^2 \zeta(3) \left(5N^2 - N N_f + \frac{3N_f}{2N} \right) \right] + O(g^6) . \end{aligned} \quad (4.18)$$

The term of order g^0 inside the square brackets represents the self-contraction of $\text{tr } a^2$, while the terms of higher order in g^2 represent the self-contractions of the operator through the interaction vertices coming from the matrix model action. Analogous expressions can be worked out for operators of higher dimension.

4.2 Correlators in the matrix model

Once the operators have been identified, their correlators can be computed in a straightforward way using the definition (4.12). In particular the two-point correlators are defined as

$$\mathcal{G}_{\vec{n},\vec{m}} = \langle \mathcal{O}_{\vec{n}}(a) \mathcal{O}_{\vec{m}}(a) \rangle = \frac{\langle e^{-S_{\text{int}}} \mathcal{O}_{\vec{n}}(a) \mathcal{O}_{\vec{m}}(a) \rangle_0}{\langle e^{-S_{\text{int}}} \rangle_0} . \quad (4.19)$$

Since normal-ordered operators with different dimensions are orthogonal to each other, $\mathcal{G}_{\vec{n},\vec{m}}$ vanishes for $n \neq m$.

For instance, for the simplest operator $\mathcal{O}_{(2)}(a)$ defined in (4.18) we find

$$\begin{aligned} \mathcal{G}_{(2),(2)} = & \frac{N^2 - 1}{2} \left[1 + \frac{g^2}{8\pi^2} 2(1 + \gamma_E)(2N - N_f) + \left(\frac{g^2}{8\pi^2} \right)^2 3(1 + \gamma_E)^2(2N - N_f)^2 \right. \\ & \left. - \left(\frac{g^2}{8\pi^2} \right)^2 \zeta(3) \left(15N^2 - 3NN_f + \frac{9N_f}{2N} \right) \right] + O(g^6) . \end{aligned} \quad (4.20)$$

The explicit expressions of correlators with higher dimensional operators can be computed in a similar way. At dimension 4 we find

$$\begin{aligned} \mathcal{G}_{(2,2),(2,2)} = & \frac{N^4 - 1}{2} \left[1 + \left(\frac{g^2}{8\pi^2} \right) 4(1 + \gamma_E)(2N - N_f) + \left(\frac{g^2}{8\pi^2} \right)^2 10(1 + \gamma_E)^2(2N - N_f)^2 \right. \\ & \left. - \left(\frac{g^2}{8\pi^2} \right)^2 12\zeta(3) \left(2N^2 - \frac{NN_f}{2} + \frac{N_f}{2N} \right) \right] \\ & - \left(\frac{g^2}{8\pi^2} \right)^2 \frac{3}{2} \zeta(3) (N^2 - 1) \left(2N^4 + 22N^2 - 3NN_f + \frac{7N_f}{N} \right) + O(g^6) , \end{aligned} \quad (4.21a)$$

$$\begin{aligned} \mathcal{G}_{(4),(2,2)} = & \frac{2N^4 - 5N^2 + 3}{2N} \left[1 + \left(\frac{g^2}{8\pi^2} \right) 4(1 + \gamma_E)(2N - N_f) \right. \\ & + \left(\frac{g^2}{8\pi^2} \right)^2 10(1 + \gamma_E)^2(2N - N_f)^2 - \left(\frac{g^2}{8\pi^2} \right)^2 12\zeta(3) \left(2N^2 - \frac{NN_f}{2} + \frac{N_f}{2N} \right) \left. \right] \\ & - \left(\frac{g^2}{8\pi^2} \right)^2 \frac{3}{2} \zeta(3) (N^2 - 1) \left(6N^3 - N^2N_f + 6N + 8N_f - \frac{21N_f}{N^2} \right) + O(g^6) , \end{aligned} \quad (4.21b)$$

$$\begin{aligned} \mathcal{G}_{(4),(4)} = & \frac{N^6 - 7N^4 + 24N^2 - 18}{4N^2} \left[1 + \left(\frac{g^2}{8\pi^2} \right) 4(1 + \gamma_E)(2N - N_f) \right. \\ & + \left(\frac{g^2}{8\pi^2} \right)^2 10(1 + \gamma_E)^2(2N - N_f)^2 - \left(\frac{g^2}{8\pi^2} \right)^2 12\zeta(3) \left(2N^2 - \frac{NN_f}{2} + \frac{N_f}{2N} \right) \left. \right] \\ & - \left(\frac{g^2}{8\pi^2} \right)^2 \frac{3}{2} \zeta(3) (N^2 - 1) \left(12N^2 + NN_f - 18 - \frac{21N_f}{N} + \frac{63N_f}{N^3} \right) + O(g^6) . \end{aligned} \quad (4.21c)$$

Here we have split the $O(g^4)$ contribution into the sum of a few terms in order to facilitate a comparison with the field theory calculation.

It is easy to check that for $N_f = 2N$ the matrix model correlators $\mathcal{G}_{\vec{n},\vec{m}}$ exactly match, up to two loops, the correlators $G_{\vec{n},\vec{m}}^R$ computed in perturbation theory (see (3.26) and

(3.27)), thus confirming the general results obtained in [8–15]⁵. The fact that the partition function on the sphere S^4 and its associated matrix model contain information on the correlators in the flat space \mathbb{R}^4 is not too surprising in the conformal case. We now want to investigate to what extent this relation holds in the non-conformal theories with $N_f \neq 2N$.

4.3 Comparison between matrix model and field theory correlators

Comparing (3.26) with (4.20), and (3.27) with (4.21), we see that they have the same structure and that many terms exactly match. However, for $N_f \neq 2N$ there are some differences in the terms proportional to $\zeta(3)$. To make the comparison simpler, it is convenient to write $\mathcal{G}_{\vec{n}, \vec{m}}$ in terms of the complex matrices φ and $\bar{\varphi}$ using the formalism introduced in Section 2. Indeed, it is possible to explicitly check that, up to two loops, the matrix model correlators (4.19) can be expressed as follows

$$\mathcal{G}_{\vec{n}, \vec{m}} = \frac{\langle e^{-\hat{V}_{\text{eff}}(\varphi, \bar{\varphi})} O_{\vec{n}}(\varphi) \bar{O}_{\vec{m}}(\bar{\varphi}) \rangle}{\langle e^{-\hat{V}_{\text{eff}}(\varphi, \bar{\varphi})} \rangle} + O(g^6), \quad (4.22)$$

where

$$\hat{V}_{\text{eff}}(\varphi, \bar{\varphi}) = -(\hat{c}_1 + \hat{c}_2) V_2(\varphi, \bar{\varphi}) - \hat{c}_3 V_4^{(B)}(\varphi, \bar{\varphi}) \quad (4.23)$$

with V_2 and $V_4^{(B)}$ defined, respectively, in (2.28) and (2.37), and

$$\begin{aligned} \hat{c}_1 &= \frac{g^2}{8\pi^2} (1 + \gamma_E)(2N - N_f), \\ \hat{c}_2 &= -3\zeta(3) \left(\frac{g^2}{8\pi^2} \right)^2 \left(2N^2 - \frac{NN_f}{2} + \frac{N_f}{2N} \right), \\ \hat{c}_3 &= 3\zeta(3) \left(\frac{g^2}{8\pi^2} \right)^2. \end{aligned} \quad (4.24)$$

Notice that the effective vertex (4.23) has the same form as the renormalized vertex (3.22) obtained from perturbation theory. Comparing (4.24) with (3.19) and (3.25), we find

$$\hat{c}_1 = c_1, \quad \hat{c}_2 = c_2 + 9\zeta(3) \left(\frac{g^2}{8\pi^2} \right)^2 N(2N - N_f), \quad \hat{c}_3 = c_3. \quad (4.25)$$

Therefore, the difference between the effective vertex \hat{V}_{eff} of the matrix model and the renormalized effective vertex V_{eff}^R is

$$\delta = \hat{V}_{\text{eff}} - V_{\text{eff}}^R = 9\zeta(3) \left(\frac{g^2}{8\pi^2} \right)^2 N(2N - N_f) V_2(\varphi, \bar{\varphi}). \quad (4.26)$$

It is interesting to observe that δ vanishes in the conformal case. Moreover, it is proportional to V_2 which, as follows from (2.29), computes the scaling dimension of the operators⁶. This

⁵In the recent paper [29] a discrepancy at six loops, proportional to $\zeta^2(5)g^{12}$, has been pointed out in the comparison between the matrix model results and the correlators obtained by solving Toda equations.

⁶Notice that a non-zero value of δ can be compensated by performing a finite renormalization of the scalar operators.

fact suggests that it might be interpreted as due to a conformal anomaly which, in non-conformal theories, affects the correlation functions in going from the four-sphere S^4 to the flat space \mathbb{R}^4 , or vice versa.

In the two-loop approximation, we can rewrite (4.22) as follows:

$$\mathcal{G}_{\vec{n},\vec{m}} = \frac{1}{(1 - \hat{c}_1 - \hat{c}_2)^n} \left[G_{\vec{n},\vec{m}}|_{\text{tree}} + \hat{c}_3 \langle V_4^{(B)}(\varphi, \bar{\varphi}) O_{\vec{n}}(\varphi) \bar{O}_{\vec{m}}(\bar{\varphi}) \rangle \right] + O(g^6) . \quad (4.27)$$

This formula clearly shows that the dependence on \hat{c}_1 and \hat{c}_2 drops out in the ratio between correlators of operators with the same scaling dimensions. Thus, in analogy with (3.29), we are led to define the ratio of correlators in the matrix model

$$\mathcal{A}_{\vec{n},\vec{m}} = \frac{\mathcal{G}_{\vec{n},\vec{m}}}{[\mathcal{G}_{(2),(2)}]^{\frac{n}{2}}} . \quad (4.28)$$

Since $\hat{c}_3 = c_3$, it exactly matches the normalized correlator $A_{\vec{n},\vec{m}}^R$, namely

$$\mathcal{A}_{\vec{n},\vec{m}} = A_{\vec{n},\vec{m}}^R . \quad (4.29)$$

We have checked this relation in many explicit examples, with operators of dimensions up to 6.

5 Two-point correlators on the four-sphere

In this section we study in more detail the relation between the correlators in flat space, discussed in Sections 2 and 3, and those on the four-sphere S^4 . The latter are closely related to the correlators derived from matrix model presented in Section 4. In particular we consider the one-loop correction to the scalar propagator on S^4 and compare it with the one-loop propagator in flat space defined in (2.12).

To this aim, it is convenient to describe a sphere in D -dimensions by using flat embedding coordinates $\{\eta_0, \eta_\mu\}$ satisfying the quadratic constraint

$$\eta_0^2 + \sum_{\mu=1}^D \eta_\mu^2 = R^2 , \quad (5.1)$$

where R is the radius of the D -sphere. Following [30–34], we use the stereographic projection

$$\eta_0 = R \frac{x^2 - R^2}{x^2 + R^2} , \quad \eta_\mu = R^2 \frac{2x_\mu}{x^2 + R^2} \quad \text{with} \quad x^2 = \sum_{\mu=1}^D x_\mu^2 , \quad (5.2)$$

to relate a theory defined on a D -sphere to a theory in \mathbb{R}^D , parametrized by the flat coordinates x_μ . One of the advantages of this formalism is that the scalar propagator on the sphere, denoted by a subscript S , takes a very simple form given by

$$\langle \varphi^a(\eta_1) \bar{\varphi}^b(\eta_2) \rangle_S = \Delta_S(\eta_{12}) \delta^{ab} , \quad (5.3)$$

where $\eta_{12} = \eta_1 - \eta_2$ and

$$\Delta_S(\eta_{12}) = \frac{\Gamma(1-\epsilon)}{4\pi (\pi\eta_{12}^2)^{1-\epsilon}} . \quad (5.4)$$

Here we have used $D = 4 - 2\epsilon$ and defined

$$\eta_{12}^2 = \frac{(x_1 - x_2)^2}{\kappa(x_1)\kappa(x_2)} , \quad \kappa(x) = \frac{x^2 + R^2}{2R^2} . \quad (5.5)$$

Inserting this into (5.4) and comparing with (2.7), we get

$$\Delta_S(\eta_{12}) = [\kappa(x_1)\kappa(x_2)]^{1-\epsilon} \Delta(x_{12}) . \quad (5.6)$$

The scalar propagator on the sphere is thus proportional to the one in flat space, with a scaling factor raised to the engineering dimensions of the scalar fields. Notice that this is the same scaling factor that defines the induced metric on the sphere through the conformal map (5.2); indeed

$$ds^2 = d\eta_0^2 + \sum_{\mu=1}^D d\eta_\mu^2 = \frac{1}{\kappa^2(x)} \sum_{\mu=1}^D dx_\mu^2 . \quad (5.7)$$

Let us now consider the correlators between two operators on the sphere. They have a structure similar to the ones in flat space given in (2.6), namely

$$\langle O_{\vec{n}}(\eta_1) \bar{O}_{\vec{m}}(\eta_2) \rangle_S = \Delta_S^n(\eta_{12}) G_{\vec{n},\vec{m}}^{(S)}(g_0, \epsilon, \eta_{12}) \delta_{nm} . \quad (5.8)$$

The correlators $G_{\vec{n},\vec{m}}^{(S)}(g_0, \epsilon, \eta_{12})$, which we will simply denote as $G_{\vec{n},\vec{m}}^{(S)}$, can be computed order by order in perturbation theory. At tree level, we have just to contract the color indices of the constituent fields, so that

$$G_{\vec{n},\vec{m}}^{(S)} \Big|_{\text{tree}} = G_{\vec{n},\vec{m}} \Big|_{\text{tree}} . \quad (5.9)$$

Inserting this into (5.8), using the propagator (5.4) and taking the limit $\epsilon \rightarrow 0$, we can easily obtain

$$\langle O_{\vec{n}}(\eta_1) \bar{O}_{\vec{m}}(\eta_2) \rangle_S \Big|_{\text{tree}} = \kappa^n(x_1) \kappa^m(x_2) \langle O_{\vec{n}}(x_1) \bar{O}_{\vec{m}}(x_2) \rangle \Big|_{\text{tree}} . \quad (5.10)$$

This is the expected relation between correlators on the sphere and correlators in flat space that follows from the conformal map (5.2).

Let us now consider the one-loop correction. Before analyzing the correlators on the sphere, it is convenient to revisit the calculation of one-loop correction to the scalar propagator in flat space, given in (2.12) in coordinate space. The one-loop correction to $\langle \varphi^a(x_1) \bar{\varphi}^b(x_2) \rangle$ can be written as

$$W_1^{ab}(x_{12}) = -g_0^2 (2N - N_f) W_1(x_{12}) \delta^{ab} , \quad (5.11)$$

where

$$W_1(x_{12}) = \int d^D x_3 d^2 \bar{\theta}_3 d^D x_4 d^2 \theta_4 \Delta(x_{13}) (e^{-2i\theta_4 \partial_{x_{43}} \bar{\theta}_3} \Delta(x_{43}))^2 \Delta(x_{42}) . \quad (5.12)$$

Its Fourier transform is the function $\mathcal{W}_1(p)$ discussed in Appendix B (see in particular (B.8) and (B.9)). Computing the integrals, we find

$$W_1(x_{12}) = -\frac{(\pi x_{12}^2)^\epsilon \Gamma(1-\epsilon)}{(4\pi)^2 \epsilon(1-2\epsilon)} \Delta(x_{12}) . \quad (5.13)$$

Using this in (5.11), one recovers the result presented in (2.12) and (2.13).

Going to the sphere, we find that the one-loop correction to the scalar propagator has a form similar to (5.11), that is

$$W_{1S}^{ab}(\eta_{12}) = -g_0^2 (2N - N_f) W_{1S}(\eta_{12}) \delta^{ab} , \quad (5.14)$$

where the function W_{1S} is the sphere generalization of W_1 . Applying the embedding formalism [30–34], the expression of W_{1S} can be obtained by performing the conformal transformation (5.2) to (5.12). Under this map, both the integration measure and the scalar propagators acquire scale factors according to

$$\begin{aligned} \int d^D x_i d^2 \theta_i &\rightarrow \int d^D x_i d^2 \theta_i \kappa^{-D+1}(x_i) , \\ \Delta(x_{ij}) &\rightarrow \Delta(x_{ij}) [\kappa(x_i) \kappa(x_j)]^{\frac{D-2}{2}} , \end{aligned} \quad (5.15)$$

so that $W_1(x_{12})$ becomes

$$W_{1S}(\eta_{12}) = [\kappa(x_1) \kappa(x_2)]^{1-\epsilon} I(x_1, x_2) , \quad (5.16)$$

where

$$I(x_1, x_2) = \int d^D x_3 d^2 \bar{\theta}_3 d^D x_4 d^2 \theta_4 \Delta(x_{13}) (e^{-2i\theta_4 \partial_{x_{43}} \bar{\theta}_3} \Delta(x_{43}))^2 \Delta(x_{42}) [\kappa(x_3) \kappa(x_4)]^{-\epsilon} . \quad (5.17)$$

Comparing this integral with (5.12), we notice the presence of the additional scaling factor $[\kappa(x_3) \kappa(x_4)]^{-\epsilon}$, which clearly becomes 1 in four dimensions.

Therefore, if the integrals in (5.12) and (5.16) were finite, W_{1S} and W_1 would only differ by the overall scaling factor $\kappa(x_1) \kappa(x_2)$. In other words, if no UV divergences are present, one can safely perform the limit $\epsilon \rightarrow 0$ inside the integrals. However, the integral in (5.17) is divergent, and thus the scaling factor $[\kappa(x_3) \kappa(x_4)]^{-\epsilon}$ in the integrand cannot be neglected. The evaluation of this integral is presented in Appendix C, and the result is

$$W_{1S}(\eta_{12}) \approx -\frac{(\pi \eta_{12}^2)^\epsilon \Gamma(1-\epsilon)}{(4\pi)^2 \epsilon(1-2\epsilon)} \Delta_S(\eta_{12}) . \quad (5.18)$$

Comparing with (5.13), we see that, up to terms $O(\epsilon)$, the two expressions coincide upon replacing Δ_S with Δ , and η_{12}^2 with x_{12}^2 . The fact that the divergent parts of W_{1S} and W_1 coincide, is not surprising since the UV divergences come from integration at short distances where there is no distinction between the sphere and flat space. What is non trivial, however, is that the finite parts coincide, modulo the obvious replacement of x_{12} with η_{12} .

Putting everything together, we see that the one-loop correction to the scalar propagator on the sphere is

$$W_{1S}^{ab}(\eta_{12}) = v_{2,1}^{(S)} \Delta_S(\eta_{12}) \delta^{ab} , \quad (5.19)$$

with

$$v_{2,1}^{(S)} \approx \frac{g_0^2}{8\pi^2} (2N - N_f) \frac{(\pi\eta_{12}^2)^\epsilon \Gamma(1 - \epsilon)}{2\epsilon(1 - 2\epsilon)} , \quad (5.20)$$

in full analogy with (2.12) and (2.13). This implies that

$$G_{\vec{n}, \vec{m}}^{(S)} \big|_{1\text{-loop}} = n v_{2,1}^{(S)} G_{\vec{n}, \vec{m}} \big|_{\text{tree}} . \quad (5.21)$$

Thus, the renormalization procedure can be done following the same steps we described in Section 3. Choosing the renormalization scale μ^2 as in (3.23) with x^2 replaced by η_{12}^2 on the sphere and by x_{12}^2 in flat space, then

$$\langle O_{\vec{n}}^R(\eta_1) \bar{O}_{\vec{m}}^R(\eta_2) \rangle_S \big|_{1\text{-loop}} = \kappa^n(x_1) \kappa^m(x_2) \langle O_{\vec{n}}^R(x_1) \bar{O}_{\vec{m}}^R(x_2) \rangle \big|_{1\text{-loop}} . \quad (5.22)$$

The relation (5.21) and the explicit expression of $v_{2,1}^{(S)}$ explain why the correlators $\mathcal{G}_{\vec{n}, \vec{m}}$ obtained from the matrix model perfectly agree with those computed in field theory at one loop.

The same analysis can be carried out at two loops, even though the resulting integrals on the sphere become way more complicated. Most of the two-loop diagrams develop UV divergences and need to be regularized. As in the one-loop case, the integrals on the sphere differ from those in flat space because of scaling factors $[\kappa(x_i)]^{-\epsilon}$ appearing in the integrands. Such factors do not modify the leading UV divergent contribution but they do affect the finite part. As a result, there is no reason *a priori* to expect that the finite part of the correlation functions on the sphere and in flat space should coincide. However, we stress the fact that the finite part of the two-point correlator is not a physical observable since it depends on the regularization scheme. The explicit one-loop calculation shows a perfect agreement between the matrix model and the field theory results for the two-point correlators for the special choice of the renormalization scale. It is natural to ask whether such identification holds also at higher loops. At two loops, the results of Sections 3 and 4 reveal that the finite part of the correlation functions are different in flat space and in the matrix model. Still, a perfect match is found for physical observables that are independent of the renormalization scheme, such as the ratios of correlators with operators of the same dimension. In such ratios, all divergent two-loop diagrams cancel and the whole contribution at order g^4 is due to a single and finite Feynman diagram, namely the irreducible diagram represented in Fig. 10. The corresponding Feynman integral is finite in \mathbb{R}^4 and does not require a regularization. As a consequence, it possesses the four-dimensional conformal symmetry and takes the same form in \mathbb{R}^4 and S^4 . This explains why the ratios of the correlation functions match the prediction from localization at two loops, as shown in (4.29).

6 Summary and conclusions

We have explicitly computed the two-point correlation functions between chiral and anti-chiral operators in the $\mathcal{N} = 2$ SYM theory with gauge group $SU(N)$ and N_f fundamental flavors up to two loops, using standard (super) Feynman diagrams in dimensional regularization. Our results show that these correlators have a remarkably simple structure of UV divergences stemming from the fact that the anomalous dimensions of the operators are proportional to the β -function. We demonstrated that when the renormalization scale μ and the separation x between the operators are inversely proportional to each other, these correlators can be obtained via a matrix model which is strikingly similar to the matrix model that computes the partition function and the chiral/anti-chiral correlators on the four-sphere using localization. Up to two loops, the difference between the two matrix models is just a term of order g^4 proportional to $(2N - n_f) V_2$, which acting on the operators gives their anomalous dimensions. This suggests that this difference that vanishes in the conformal theories, might be interpreted as a conformal anomaly. In the non-conformal cases this could explain the difference between the correlators on the four-sphere and those in flat space.

We have also constructed normalized correlators, which are scheme independent and, as such, represent physical quantities. Up to two-loops, these normalized correlators are the same on the four-sphere and in flat space, and can be computed either using the field theory approach with Feynman diagrams, or using localization methods via a simple matrix model.

Our analysis clarifies the relation between the perturbative field calculations and the localization results in $\mathcal{N} = 2$ SYM theories. It would be interesting to generalize it in various directions, for example to compute the correlators at three or more loops, or to compute the one-point or higher-point correlation functions in presence of Wilson loops. In particular it would be interesting to explore in detail the two-loop calculations of the correlators using Feynman diagrams on the sphere, and/or obtain a “first-principle” derivation of the difference between the two matrix models that yield the correlators on the four-sphere and in flat space. We hope to be able to return to some of these points in future works.

Acknowledgments

We would like to thank A. Belitsky, L. Bianchi, M. Frau, R. Frezzotti, F. Galvagno, P. Gregori, K. Papadodimas, N. Tantalò and T. Vladikas for many useful discussions.

The work of M.B., A.L., F.F., J.F.M. is partially supported by the MIUR PRIN Contract 2015MP2CX4 “Non-perturbative Aspects Of Gauge Theories And Strings”. The work of G.P.K. is supported by the French National Agency for Research grant ANR-17-CE31-0001-01. The work of A.L. is partially supported by the “Fondi Ricerca Locale dell’Università del Piemonte Orientale”. All authors would like thank the Galileo Galilei Institute for Theoretical Physics for hospitality during the course of this work. G.P.K. is grateful to INFN and the Simons Foundation for partial support.

A Loop integrals

In this appendix we follow closely [17] (see also [18] for a review) and collect some useful formulae necessary to evaluate the Feynman integrals. We work in $D = 4 - 2\epsilon$ dimensions and use the propagator of a massless scalar field given in (2.7), namely

$$\Delta(x) = \int \frac{d^D k}{(2\pi)^D} \frac{e^{ik \cdot x}}{k^2} = \frac{\Gamma(1 - \epsilon)}{(4\pi) (\pi x^2)^{1-\epsilon}} . \quad (\text{A.1})$$

For later convenience, we introduce the graphical notation for Feynman integrals in the momentum representation

$$\begin{array}{c} \alpha \\ \circlearrowleft \\ \beta \end{array} \equiv \int \frac{d^D k}{(2\pi)^D} \frac{1}{(k^2)^\alpha ((p-k)^2)^\beta} = \frac{I_{\alpha,\beta}}{(p^2)^{\alpha+\beta-2+\epsilon}} , \quad (\text{A.2})$$

where

$$I_{\alpha,\beta} = \frac{\Gamma(2 - \epsilon - \alpha) \Gamma(2 - \epsilon - \beta) \Gamma(\alpha + \beta - 2 + \epsilon)}{(4\pi)^{2-\epsilon} \Gamma(\alpha) \Gamma(\beta) \Gamma(4 - 2\epsilon - \alpha - \beta)} . \quad (\text{A.3})$$

The black dots on the left and the right of the diagram in (A.2) denote, respectively, the incoming and outgoing momentum p . Furthermore, in each interaction vertex the momentum conservation is enforced. When α or β is 1, for simplicity we do not write the labels. With these notations, we then have

$$\begin{array}{c} \circlearrowleft \end{array} = \frac{\Gamma^2(1 - \epsilon) \Gamma(\epsilon)}{(4\pi)^{2-\epsilon} \Gamma(2 - 2\epsilon)} \frac{1}{(p^2)^\epsilon} . \quad (\text{A.4})$$

We will also make use of the Fourier transform integral

$$\Pi_\alpha(x) = \int \frac{d^D k}{(2\pi)^D} \frac{e^{ik \cdot x}}{(k^2)^\alpha} = \frac{(x^2)^{\alpha+\epsilon-2} \Gamma(2 - \epsilon - \alpha)}{4^\alpha \pi^{2-\epsilon} \Gamma(\alpha)} = \frac{(x^2)^{\alpha-1} \Gamma(2 - \epsilon - \alpha)}{4^{\alpha-1} \Gamma(\alpha) \Gamma(1 - \epsilon)} \Delta(x) , \quad (\text{A.5})$$

which for $\alpha = 1$ reduces to (A.1). In particular we will need the following explicit formulae

$$\Pi_{1+\epsilon}(x) = \frac{(x^2)^\epsilon \Gamma(1 - 2\epsilon)}{4^\epsilon \Gamma(1 + \epsilon) \Gamma(1 - \epsilon)} \Delta(x) , \quad (\text{A.6a})$$

$$\Pi_{1+2\epsilon}(x) = \frac{(x^2)^{2\epsilon} \Gamma(1 - 3\epsilon)}{4^{2\epsilon} \Gamma(1 + 2\epsilon) \Gamma(1 - \epsilon)} \Delta(x) , \quad (\text{A.6b})$$

$$\Pi_{3\epsilon}(x) = \frac{(x^2)^{2\epsilon} \Gamma(2 - 4\epsilon)}{4^{3\epsilon-2} \pi^{\epsilon-2} \Gamma(3\epsilon) \Gamma(1 - \epsilon)^2} \Delta^2(x) . \quad (\text{A.6c})$$

A.1 Triangle identity

Let us consider the integral

$$J(\{\alpha_i\}) = \int \frac{d^D k}{(2\pi)^D} \frac{1}{(k^2)^{\alpha_1} ((k-q)^2)^{\alpha_2} ((k-p)^2)^{\alpha_3} (q^2)^{\alpha_4} ((q-p)^2)^{\alpha_5} (p^2)^{\alpha_6}} , \quad (\text{A.7})$$

which corresponds to the triangle diagram of Fig. 11.

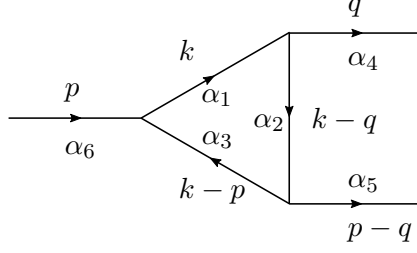


Figure 11. The one-loop diagram corresponding to the integral (A.7). Here the labels α_i on the various lines denote the exponents of the propagators appearing in the integrand.

Following [17, 18], we have

$$\begin{aligned}
0 &= \int \frac{d^D k}{(2\pi)^D} \frac{\partial}{\partial k^\mu} \left[\frac{(k-q)^\mu}{(k^2)^{\alpha_1} ((k-q)^2)^{\alpha_2} ((k-p)^2)^{\alpha_3} (q^2)^{\alpha_4} ((q-p)^2)^{\alpha_5} (p^2)^{\alpha_6}} \right] \\
&= \int \frac{d^D k}{(2\pi)^D} \frac{D - \alpha_1 \frac{2k \cdot (k-q)}{k^2} - 2\alpha_2 - \alpha_3 \frac{2(k-p) \cdot (k-q)}{(k-p)^2}}{(k^2)^{\alpha_1} ((k-q)^2)^{\alpha_2} ((k-p)^2)^{\alpha_3} (q^2)^{\alpha_4} ((q-p)^2)^{\alpha_5} (p^2)^{\alpha_6}} \\
&= \int \frac{d^D k}{(2\pi)^D} \frac{D - \alpha_1 - \alpha_1 \frac{(k-q)^2 - q^2}{k^2} - 2\alpha_2 - \alpha_3 - \alpha_3 \frac{(k-q)^2 - (q-p)^2}{(k-p)^2}}{(k^2)^{\alpha_1} ((k-q)^2)^{\alpha_2} ((k-p)^2)^{\alpha_3} (q^2)^{\alpha_4} ((q-p)^2)^{\alpha_5} (p^2)^{\alpha_6}}.
\end{aligned} \tag{A.8}$$

From this, it is easy to obtain the so-called triangle identity:

$$(D - \alpha_1 - 2\alpha_2 - \alpha_3) J(\{\alpha_i\}) = \left[\alpha_1 \mathbf{1}^+ (\mathbf{2}^- - \mathbf{4}^-) + \alpha_3 \mathbf{3}^+ (\mathbf{2}^- - \mathbf{5}^-) \right] J(\{\alpha_i\}), \tag{A.9}$$

where the notation $\mathbf{n}^\pm J(\{\alpha_i\})$ means the integral (A.7) with α_n replaced by $\alpha_n \pm 1$. For example, we have

$$\mathbf{1}^+ \mathbf{2}^- J(\{\alpha_i\}) = \int \frac{d^D k}{(2\pi)^D} \frac{1}{(k^2)^{\alpha_1+1} ((k-q)^2)^{\alpha_2-1} ((k-p)^2)^{\alpha_3} (q^2)^{\alpha_4} ((q-p)^2)^{\alpha_5} (p^2)^{\alpha_6}}. \tag{A.10}$$

Repeated applications of the triangle identity allow us to reduce the power of one of the propagators to zero and to express in the end the result in terms of the basic integrals (A.2). A few examples are described in the next subsection.

A.2 Scalar integrals

Let us consider the two-loop integral

$$\int \frac{d^D k d^D q}{(2\pi)^{2D}} \frac{1}{k^2 (k-q)^2 (k-p)^2 q^2 (q-p)^2} \equiv \text{Diagram} \tag{A.11}$$

Here we have adopted the same graphical conventions as in (A.4).

Applying the triangle identity (A.9), we obtain

$$\text{Diagram 1} = \frac{1}{\epsilon} \left[\text{Diagram 2} - \text{Diagram 3} \right], \quad (\text{A.12})$$

where

$$\text{Diagram 2} \equiv \int \frac{d^D k d^D q}{(2\pi)^{2D}} \frac{1}{(k^2)^2 (k-q)^2 (k-p)^2 (q-p)^2} = \frac{I_{1,1} I_{2,1+\epsilon}}{(p^2)^{1+2\epsilon}}, \quad (\text{A.13a})$$

$$\text{Diagram 3} \equiv \int \frac{d^D k d^D q}{(2\pi)^{2D}} \frac{1}{(k^2)^2 (k-p)^2 q^2 (q-p)^2} = \frac{I_{2,1} I_{1,1}}{(p^2)^{1+2\epsilon}}. \quad (\text{A.13b})$$

The last steps in these equations follow from (A.2). Inserting these expressions into (A.12) and expanding for $\epsilon \rightarrow 0$, we obtain

$$\text{Diagram 1} = \frac{I_{1,1} [I_{2,1+\epsilon} - I_{2,1}]}{\epsilon} \frac{1}{(p^2)^{1+2\epsilon}} = \frac{6\zeta(3)}{(4\pi)^4} \frac{1}{(p^2)^{1+2\epsilon}} + \dots. \quad (\text{A.14})$$

After Fourier transforming and using (A.6b), we get

$$\text{Diagram 1} \rightarrow \frac{6\zeta(3)}{(4\pi)^4} \Pi_{1+2\epsilon}(x) + \dots = \frac{6\zeta(3)}{(4\pi)^4} (\pi x^2)^{2\epsilon} \Delta(x) + \dots. \quad (\text{A.15})$$

The same procedure can be applied to express other two-loop integrals in terms of $I_{\alpha,\beta}$ defined in (A.3). For example, we have

$$\text{Diagram 4} = \frac{I_{1,1} I_{1,2} [I_{1+\epsilon,1+\epsilon} - I_{1,1+2\epsilon}]}{\epsilon} \frac{1}{(p^2)^{3\epsilon}} = \frac{2\zeta(3)}{\epsilon (4\pi)^6} \frac{1}{(p^2)^{3\epsilon}} + \dots. \quad (\text{A.16})$$

Computing the Fourier transform and using (A.6c), we find

$$\text{Diagram 4} \rightarrow \frac{2\zeta(3)}{\epsilon (4\pi)^6} \Pi_{3\epsilon}(x) + \dots = \frac{6\zeta(3)}{(4\pi)^4} (\pi x^2)^{2\epsilon} \Delta(x)^2 + \dots. \quad (\text{A.17})$$

Another scalar integral that will be needed is the one represented by the diagram

$$p^2 \text{Diagram 5}. \quad (\text{A.18})$$

Using (A.4) and expanding for small ϵ , one can prove that

$$\text{Diagram 5} = \frac{I_{1,1}}{(p^2)^\epsilon} \text{Diagram 1} + \dots = \frac{6\zeta(3)}{\epsilon (4\pi)^6} \frac{1}{(p^2)^{1+3\epsilon}} + \dots \quad (\text{A.19})$$

where the ellipses stand for terms that vanish for $\epsilon \rightarrow 0$. Comparing with (A.16), we easily conclude that

$$p^2 \text{ (circle with vertical line and dots) } = 3 \text{ (circle with horizontal line and dots) } + \dots \quad (\text{A.20})$$

so that, after Fourier transform, we have

$$p^2 \text{ (circle with vertical line and dots) } \longrightarrow \frac{18\zeta(3)}{(4\pi)^4} (\pi x^2)^{2\epsilon} \Delta(x)^2 + \dots \quad (\text{A.21})$$

In a similar way one can derive the following relation

$$\text{ (circle with vertical line and dots) } = \frac{I_{1,1}}{(p^2)^\epsilon} \text{ (circle with vertical line and dots) } + \dots = \frac{6\zeta(3)}{\epsilon (4\pi)^6} \frac{1}{(p^2)^{1+3\epsilon}} + \dots \quad (\text{A.22})$$

from which we get

$$p^2 \text{ (circle with vertical line and dots) } = 3 \text{ (circle with horizontal line and dots) } + \dots \quad (\text{A.23})$$

Performing the Fourier transform we obtain

$$p^2 \text{ (circle with vertical line and dots) } \longrightarrow \frac{18\zeta(3)}{(4\pi)^4} (\pi x^2)^{2\epsilon} \Delta(x)^2 + \dots \quad (\text{A.24})$$

The following divergent integrals also appear in the two-loop calculation

$$\frac{1}{p^2} \text{ (circle with dots) } = \frac{I_{1,1}}{(p^2)^{1+\epsilon}} = \frac{\Gamma^2(1-\epsilon) \Gamma(\epsilon)}{(4\pi)^{2-\epsilon} \Gamma(2-2\epsilon)} \frac{1}{(p^2)^{1+\epsilon}}, \quad (\text{A.25a})$$

$$\text{ (two circles connected by a line) } = \frac{I_{1,1}^2}{(p^2)^{1+2\epsilon}} = \left[\frac{\Gamma^2(1-\epsilon) \Gamma(\epsilon)}{(4\pi)^{2-\epsilon} \Gamma(2-2\epsilon)} \right]^2 \frac{1}{(p^2)^{1+2\epsilon}}, \quad (\text{A.25b})$$

$$\frac{1}{p^2} \text{ (circle with vertical line and dots) } = \frac{I_{1,1} I_{1,1+\epsilon}}{(p^2)^{1+2\epsilon}} = \frac{\Gamma^3(1-\epsilon) \Gamma(2\epsilon)}{(4\pi)^{4-2\epsilon} \epsilon (1-2\epsilon) \Gamma(2-3\epsilon)} \frac{1}{(p^2)^{1+2\epsilon}}, \quad (\text{A.25c})$$

$$\text{ (circle with horizontal line and dots) } = \frac{I_{1,1} I_{1,2+\epsilon}}{(p^2)^{1+2\epsilon}} = -\frac{\Gamma^3(1-\epsilon) \Gamma(2\epsilon)}{(4\pi)^{4-2\epsilon} \epsilon (1-2\epsilon) (1+\epsilon) \Gamma(1-3\epsilon)} \frac{1}{(p^2)^{1+2\epsilon}}, \quad (\text{A.25d})$$

$$\text{ (circle with horizontal line and dots) } = \frac{I_{1,1}^2 I_{\epsilon,2+\epsilon}}{(p^2)^{3\epsilon}} = -\frac{\Gamma^4(1-\epsilon) \Gamma(3\epsilon)}{2(4\pi)^{6-3\epsilon} \epsilon^2 (1-2\epsilon) (1+\epsilon) \Gamma(2-4\epsilon)} \frac{1}{(p^2)^{3\epsilon}}. \quad (\text{A.25e})$$

After Fourier transforming, we get using (A.6)

$$\frac{1}{p^2} \text{ (bubble diagram) } \longrightarrow I_{1,1} \Pi_{1+\epsilon}(x) = \frac{(\pi x^2)^\epsilon \Gamma(1-\epsilon)}{(4\pi)^2 (1-2\epsilon)} \Delta(x) , \quad (\text{A.26a})$$

$$\text{Diagram: two circles connected by a horizontal line, with a black dot on each circle} \longrightarrow I_{1,1}^2 \Pi_{1+2\epsilon}(x) = \left[\frac{(\pi x^2)^\epsilon \Gamma(1-\epsilon)}{(4\pi)^2 \epsilon(1-2\epsilon)} \right]^2 \Delta(x) + O(\epsilon) \ , \quad (\text{A.26b})$$

$$\frac{1}{p^2} \text{ (diagram of a circle with two vertices and a chord)} \longrightarrow I_{1,1} I_{1,1+\epsilon} \Pi_{1+2\epsilon}(x) = \frac{(\pi x^2)^{2\epsilon} \Gamma^2(1-\epsilon)}{2(4\pi)^4 \epsilon^2(1-2\epsilon)(1-3\epsilon)} \Delta(x), \quad (\text{A.26c})$$

$$\text{Diagram} \longrightarrow I_{1,1} I_{1,2+\epsilon} \Pi_{1+2\epsilon}(x) = -\frac{(\pi x^2)^{2\epsilon} \Gamma^2(1-\epsilon)}{2(4\pi)^4 \epsilon^2(1-2\epsilon)(1+\epsilon)} \Delta(x), \quad (\text{A.26d})$$

$$\text{Diagram} \longrightarrow I_{1,1}^2 I_{\epsilon,2+\epsilon} \Pi_{3\epsilon}(x) = -\frac{(\pi x^2)^{2\epsilon} \Gamma^2(1-\epsilon)}{2(4\pi)^4 \epsilon^2(1-2\epsilon)(1+\epsilon)} \Delta(x)^2. \quad (\text{A.26e})$$

B Evaluation of the relevant (super)diagrams

In this appendix we explicitly compute the diagrams discussed in Section 2. We use dimensional regularization and the $\mathcal{N} = 1$ superspace formalism in the Feynman gauge (we refer to [15] for more details).

B.1 Feynman rules

We first summarize the momentum-space Feynman rules in the chosen formalism. Let us start from the propagators for the chiral multiplets. We use a continuous line for the superfields Φ_I ($I = 1, 2, 3$) of the $\mathcal{N} = 4$ gauge multiplet, which carry $\text{SU}(N)$ adjoint indices a, b, \dots , a dashed line for the superfields Q_A ($A = 1, \dots, N_f$), which carry $\text{SU}(N)$ fundamental indices u, v, \dots , and a dotted line for the superfields \tilde{Q}_A , also carrying fundamental indices, which form a $\mathcal{N} = 2$ hypermultiplet together with Q_A . We have

$$\frac{a, I}{\theta_1, \bar{\theta}_1} \xrightarrow{k} \frac{b, J}{\theta_2, \bar{\theta}_2} = \delta^{ab} \delta^{IJ} e^{-\theta_1 k \bar{\theta}_1 - \theta_2 k \bar{\theta}_2 + 2\theta_1 k \bar{\theta}_2} \frac{1}{k^2}, \quad (\text{B.1a})$$

$$\frac{u, A}{\theta_1, \bar{\theta}_1} \longrightarrow \frac{k}{\theta_2, \bar{\theta}_2} \frac{v, B}{\theta_2, \bar{\theta}_2} = \delta^{uv} \delta^{AB} e^{-\theta_1 k \bar{\theta}_1 - \theta_2 k \bar{\theta}_2 + 2\theta_1 k \bar{\theta}_2} \frac{1}{k^2}, \quad (\text{B.1b})$$

$$\begin{array}{c} u, A \qquad \qquad \qquad k \qquad \qquad \qquad v, B \\ \hline \theta_1, \bar{\theta}_1 \qquad \qquad \qquad \theta_2, \bar{\theta}_2 \end{array} = \delta^{uv} \delta^{AB} e^{-\theta_1 k \bar{\theta}_1 - \theta_2 k \bar{\theta}_2 + 2\theta_1 k \bar{\theta}_2} \frac{1}{k^2} . \quad (\text{B.1c})$$

Note that the arrow indicates both the orientation of the chiral propagator and the flow of the momentum. In (B.1a) we have used the notation

$$\theta k \bar{\theta} = \theta^T \sigma^\mu \bar{\theta} k_\mu = \theta^\alpha (\sigma^\mu)_{\alpha\dot{\beta}} \bar{\theta}^{\dot{\beta}} k_\mu. \quad (\text{B.2})$$

Our conventions on spinor indices and Pauli matrices are the same as those explained in Appendix A of [15].

The propagator for the $\mathcal{N} = 1$ vector superfield is given by

$$\begin{array}{c} a \\ \text{~~~~~} \xrightarrow{k} \text{~~~~~} b \\ \text{~~~~~} \end{array} = -\frac{\delta^{ab}}{2} \theta_{12}^2 \bar{\theta}_{12}^2 \frac{1}{k^2}, \quad (\text{B.3})$$

where $\theta_{12} \equiv \theta_1 - \theta_2$.

The diagrams we have to compute only contain three-point vertices. These are given by the following rules:

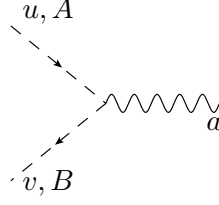
$$\begin{array}{c} a, I \\ \swarrow \\ \text{---} \\ \searrow \\ b, J \end{array} \text{---} c, K = \frac{1}{3!} \epsilon_{IJK} \sqrt{2} g_0 \theta^2 (T^a)^{bc} , \quad (\text{B.4a})$$

$$\begin{array}{c} a, I \\ \swarrow \\ \text{---} \\ \searrow \\ b, J \end{array} \rightarrow c, K = -\frac{1}{3!} \epsilon_{IJK} \sqrt{2} g_0 \bar{\theta}^2 (T^a)^{bc} , \quad (\text{B.4b})$$

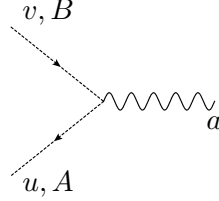
$$\begin{array}{c} u, A \\ \swarrow \\ \text{---} \\ \searrow \\ v, B \end{array} \leftarrow a, I = -i \delta_{AB} \delta_{I1} \sqrt{2} g_0 \theta^2 (T^a)_{uv} , \quad (\text{B.4c})$$

$$\begin{array}{c} v, B \\ \diagdown \\ \text{---} \\ \diagup \\ u, A \end{array} \rightarrow a, I \quad = \text{i} \delta_{AB} \delta_{I1} \sqrt{2} g_0 \bar{\theta}^2 (T^a)_{uv} \, , \quad (\text{B.4d})$$

$$\begin{array}{c} b, I \\ \swarrow \\ \searrow \\ c, J \end{array} = \delta_{IJ} 2g_0 (T^a)^{bc}, \quad (\text{B.4e})$$



$$= \delta_{AB} 2g_0 (T^a)_{uv} , \quad (\text{B.4f})$$

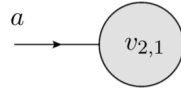


$$= -\delta_{AB} 2g_0 (T^a)_{uv} . \quad (\text{B.4g})$$

Here $(T^a)^{bc} = -i f^{abc}$ are the generators in the adjoint representation, and $(T^a)_{uv}$ those in the fundamental representation. The θ variables appearing in the vertices are those associated to the vertex point.

B.2 One-loop diagrams

At one loop, we have to compute the diagrams in Fig. 4. Denoting



$$= W_1^{ab}(x) \quad (\text{B.5})$$

and isolating a prefactor containing the combinatorial and color factors, we have

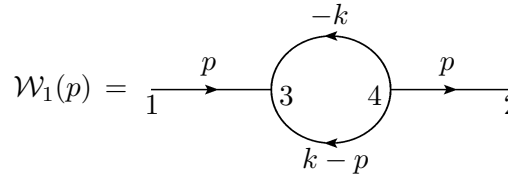
$$\begin{aligned} W_1^{ab}(x) &= (\sqrt{2}g_0)^2 (N_f \text{tr} T^a T^b - \text{tr}_{\text{adj}} T^a T^b) W_1(x) \\ &= g_0^2 (N_f - 2N) W_1(x) \delta^{ab} , \end{aligned} \quad (\text{B.6})$$

where $W_1(x)$ is given by the one-loop Feynman diagram shown in (B.8) below. The first term in the color factor arises from the loop diagram of N_f fundamental Q, \tilde{Q} superfields, while the second term originates from the loop of the adjoint hypermultiplet H .

It is convenient to Fourier transform $W_1(x)$ and write

$$W_1(x) = \int \frac{d^D p}{(2\pi)^D} \mathcal{W}_1(p) e^{ip \cdot x} , \quad (\text{B.7})$$

where $\mathcal{W}_1(p)$ is described by the following diagram in the momentum space:



$$\mathcal{W}_1(p) = \quad . \quad (\text{B.8})$$

Here the numbers label the external points and the interaction vertices. Note that the two external points 1 and 2 are connected to a bosonic scalar field, so that the propagators from

1 to 3 and from 4 to 2 are in fact free scalar propagators with no θ dependence. Taking into account the Feynman rules given above, we get

$$\begin{aligned}\mathcal{W}_1(p) &= \int \frac{d^D k}{(2\pi)^D} \frac{1}{p^4 k^2 (k-p)^2} \int d^2 \bar{\theta}_3 d^2 \theta_4 e^{-2\theta_4 p \bar{\theta}_3} \\ &= -\frac{1}{p^2} \int \frac{d^D k}{(2\pi)^D} \frac{1}{k^2 (k-p)^2} = -\frac{1}{p^2} \text{ (loop diagram) } .\end{aligned}\quad (\text{B.9})$$

In the second step we used the Grassmann integral identity

$$\int d^2 \theta_1 d^2 \bar{\theta}_2 e^{\alpha \theta_1 k \bar{\theta}_2} = -\frac{\alpha^2}{4} k^2 , \quad (\text{B.10})$$

and then we exploited the graphical representation introduced in Appendix A. Using (A.25a) and the Fourier transform (A.26a), we finally obtain

$$W_1(x) = -\frac{(\pi x^2)^\epsilon \Gamma(1-\epsilon)}{(4\pi)^2 \epsilon(1-2\epsilon)} \Delta(x) , \quad (\text{B.11})$$

leading to the relation (2.13) in the main text:

$$W_1^{ab}(x) = \frac{g_0^2}{8\pi^2} (2N - N_f) \frac{(\pi x^2)^\epsilon \Gamma(1-\epsilon)}{2\epsilon(1-2\epsilon)} \Delta(x) \delta^{ab} \equiv v_{2,1} \Delta(x) \delta^{ab} . \quad (\text{B.12})$$

B.3 Two-loop diagrams

At two loops we have to compute diagrams that correct either a two-point or a four-point vertex. Such diagrams have been displayed in Section 2. All of them have two external points, corresponding to the positions of the two operators $O_{\vec{n}}(x)$ and $\bar{O}_{\vec{m}}(0)$, four internal points, corresponding to the interaction vertices, and either seven or eight propagators, for the corrections to the two-point or the four-point vertex respectively.

Some notations

It is useful to introduce some notation that allows us to write the various diagrams in a uniform way. In each two-loop diagram labeled by an index I , we label by $i = 1, 2$ the external points and by $i = 3, \dots, 6$ the internal ones. We denote by \mathcal{E}_I the set of propagators of the diagram, and label each propagator in \mathcal{E}_I by s . Any propagator connects a point i to a point j , and in general there can be a number $r(i, j)$ of propagators connecting the same two points. A possible way of expressing the label s of the propagators is thus

$$s \rightarrow (i, j; r) \quad (\text{B.13})$$

where $r = 1, \dots, r(i, j)$; in the following we will omit the index r if $r(i, j) = 1$. The momentum k_s associated to the propagator will then be denoted as $k_{ij;r}$, with the convention that we take it to flow from i to j . This is useful to write the delta-functions of momentum conservation at internal vertices, which take the form

$$\delta_{\text{int}}(k) \equiv \prod_{i=3}^6 \delta^D \left(\sum_j \sum_{r=1}^{r(i,j)} k_{ij;r} \right) . \quad (\text{B.14})$$

Similarly, the relation between the internal momenta and the external momentum p is enforced by

$$\delta_{\text{ext}}(p, k) \equiv \delta^D \left(p - \sum_j \sum_{r=1}^{r(1,j)} k_{1j} \right) . \quad (\text{B.15})$$

Just as in the one-loop case, any two-loop diagram will be written as the product of a factor containing the weights in the vertices, the combinatorial and color factors, and of a colorless diagram $W_I(x)$, which we will obtain from its Fourier transform $\mathcal{W}_I(p)$. The latter has the following structure

$$\mathcal{W}_I(p) = \int \prod_{s \in \mathcal{E}_I} \frac{dk_s}{(2\pi)^D} \mathcal{Y}_I(p, k) \mathcal{Z}_I(p, k) , \quad (\text{B.16})$$

where

$$\begin{aligned} \mathcal{Y}_I(p, k) &= \prod_{s \in \mathcal{E}_I} \frac{1}{k_s^2} \delta_{\text{int}}(k) \delta_{\text{ext}}(p, k) , \\ \mathcal{Z}_I(p, k) &= \int \prod_{i=3}^6 d^2\theta_i d^2\bar{\theta}_i \mathfrak{D}_I(p, k, \theta, \bar{\theta}) . \end{aligned} \quad (\text{B.17})$$

The factor \mathcal{Y}_I contains the contribution of the propagators and the conditions for the momentum conservation at each vertex of the I -th diagram, while the factor $\mathfrak{D}_I(p, k, \theta, \bar{\theta})$ contains all θ and $\bar{\theta}$ terms coming from the vertices and from the superfield propagators. Some of the Grassmann integrations yielding might be obvious, in which case we will indicate only the non-trivial integrals and denote the integrand of \mathcal{Z}_I as $\tilde{\mathfrak{D}}_I$.

Reducible diagrams

The reducible two-loop diagrams are represented in Fig. 5 and Fig. 6. In the diagrams of Fig. 5 there are two independent one-loop corrections to a propagator line. Hence the result follows simply from the one-loop computation presented in the previous subsection, and has been given in (2.15) of the main text.

Let us consider then the diagrams of Fig. 6. The overall factors are simply the square of those of (B.6), and thus we get

$$\begin{array}{c} a \longrightarrow \text{---} \bigcirc \text{---} \bigcirc \text{---} b \\ \text{---} v_{2,1} \text{---} v_{2,1} \text{---} \end{array} = g_0^4 (N_f - 2N)^2 W_2(x) \delta^{ab} . \quad (\text{B.18})$$

The Fourier transform of $W_2(x)$ is given by the diagram

$$\mathcal{W}_2(p) = \begin{array}{c} \text{---} 1 \text{---} \text{---} \bigcirc \text{---} \bigcirc \text{---} \text{---} 2 \\ \text{---} k_{13} \text{---} 3 \text{---} 4 \text{---} k_{45} \text{---} 5 \text{---} 6 \text{---} k_{62} \end{array} . \quad (\text{B.19})$$

$k_{43;1}$ (top left loop), $k_{43;2}$ (bottom left loop), $k_{65;1}$ (top right loop), $k_{65;2}$ (bottom right loop)

According to the conventions described earlier, the labeling of the momenta is determined by that of the vertices. In the following, therefore, in drawing momentum space diagrams

we will only exhibit the labeling of the vertices. This diagram can be expressed in the form (B.16), with

$$\mathcal{Z}_2(p, k) = \int d^2\bar{\theta}_3 d^2\theta_4 d^2\bar{\theta}_5 d^2\theta_6 \tilde{\mathfrak{D}}_2 , \quad (\text{B.20})$$

where

$$\begin{aligned} \tilde{\mathfrak{D}}_2 &= \exp \left(2\theta_4(k_{43;1} + k_{43;2})\bar{\theta}_3 + 2\theta_6(k_{65;1} + k_{65;2})\bar{\theta}_5 + 2\theta_4 k_{45}\bar{\theta}_5 \right) \\ &= \exp \left(-2\theta_4 p \bar{\theta}_3 - 2\theta_6 p \bar{\theta}_5 + 2\theta_4 p \bar{\theta}_5 \right) . \end{aligned} \quad (\text{B.21})$$

In the second step we used the momentum conservation δ -functions that are present in the factor \mathcal{Y} defined in (B.16). Performing the Grassmann integrals, one finds $\mathcal{Z}_2(p, k) = p^4$. This factor cancels the two “external” propagators in \mathcal{Y}_2 and the integral over internal momenta can be represented in the graphical notation of Appendix A as follows:

$$\mathcal{W}_2(p) = \text{---} \bullet \text{---} \bigcirc \text{---} \bigcirc \text{---} \bullet \text{---} . \quad (\text{B.22})$$

Taking the Fourier transform of this expression via (A.26b) and inserting it into (B.18), we finally find

$$\begin{aligned} a \longrightarrow \text{---} \bigcirc_{v_{2,1}} \text{---} \bigcirc_{v_{2,1}} \text{---} b &= g_0^4 (2N - N_f)^2 \left[\frac{(\pi x^2)^\epsilon \Gamma(1 - \epsilon)}{(4\pi)^2 \epsilon (1 - 2\epsilon)} \right]^2 \Delta(x) \delta^{ab} + O(\epsilon) \\ &= v_{2,1}^2 \Delta(x) \delta^{ab} + O(\epsilon) , \end{aligned} \quad (\text{B.23})$$

in agreement with the formula (2.16) in the main text.

Irreducible diagrams: the $v_{2,2}$ part

Let us now consider the irreducible two-loop corrections to the scalar propagator, namely the diagrams represented in Fig. 8. We start from

$$\begin{aligned} W_3^{ab}(x) &\equiv \frac{a}{x} \longrightarrow \text{---} \bigcirc \text{---} \frac{b}{0} \\ &= \frac{1}{2} (\sqrt{2}g_0)^2 (2g_0)^2 (N_f \text{tr} T^a T^c T^b T^c - \text{tr}_{\text{adj}} T^a T^c T^b T^c) W_3(x) \\ &= -2g_0^4 \left(\frac{N_f}{2N} + N^2 \right) W_3(x) \delta^{ab} . \end{aligned} \quad (\text{B.24})$$

In momentum space, we have to compute

$$\mathcal{W}_3(p) = \text{---} 1 \longrightarrow 3 \text{---} \bigcirc \text{---} 4 \longrightarrow 2 \quad (\text{B.25})$$

5
6

which has the general form (B.16). The θ -factors present in the two chiral vertices saturate the integrations over θ_3 and $\bar{\theta}_4$, while those in the gluon propagator set θ_6 and $\bar{\theta}_6$ equal to θ_5 and $\bar{\theta}_5$ respectively. The remaining Grassmann integrations are

$$\mathcal{Z}_3(p, k) = \int d^2\bar{\theta}_3 d^2\theta_4 d^2\theta_5 d^2\bar{\theta}_5 \tilde{\mathfrak{D}}_3 \quad (\text{B.26})$$

with

$$\begin{aligned} \tilde{\mathfrak{D}}_3 &= \exp(-\theta_5(k_{53} + k_{63} + k_{45} + k_{46})\bar{\theta}_5 + 2\theta_5(k_{53} + k_{63})\bar{\theta}_3 + 2\theta_4(k_{45} + k_{46})\bar{\theta}_5) \\ &= \exp(2\theta_5 p \bar{\theta}_5 - 2\theta_5 p \bar{\theta}_3 - 2\theta_4 p \bar{\theta}_5) , \end{aligned} \quad (\text{B.27})$$

where in the second step we used momentum conservation. Performing the θ -integrals, we get $\mathcal{Z}_3(p, k) = p^4$, which cancels the two “external” propagators in \mathcal{Y}_3 ; the remaining integral over internal momenta can be represented in the graphical notation of Appendix A as follows:

$$\mathcal{W}_3(p) = \text{Diagram: a circle with a vertical line through its center, and two dots on the horizontal line at the left and right edges.} \quad (\text{B.28})$$

Taking the Fourier transform via (A.15), and inserting the result into (B.24), we obtain

$$W_3^{ab}(x) = -\left(\frac{g_0^2}{8\pi^2}\right)^2 3\zeta(3) \left(\frac{N_f}{2N} + N^2\right) (\pi x^2)^{2\epsilon} \Delta(x) \delta^{ab} + \dots \quad (\text{B.29})$$

Let us now consider the diagram

$$\begin{aligned} W_4^{ab}(x) &\equiv \text{Diagram: a circle with a wavy line on the right side, and two external lines on the left and right. The left line is labeled 'a' and 'x', and the right line is labeled 'b' and '0'.} \quad (\text{B.30}) \\ &= 4 \times \frac{1}{2} (\sqrt{2}g_0)^2 (2g_0)^2 (N_f \text{tr } T^a T^d T^c - \text{tr}_{\text{adj}} T^a T^d T^c) (T^c)^{db} W_4(x) . \end{aligned}$$

Using the relations

$$\text{tr } T^a T^d T^c = \frac{1}{4} (d^{adc} + i f^{adc}) , \quad \text{tr}_{\text{adj}} T^a T^d T^c = i \frac{N}{2} f^{adc} \quad (\text{B.31})$$

we get

$$\begin{aligned} W_4^{ab}(x) &= 4g_0^4 (N_f (d^{adc} + i f^{adc}) - 2N i f^{adc}) i f^{cdb} W_4(x) \\ &= -4g_0^4 N (2N - N_f) W_4(x) \delta^{ab} , \end{aligned} \quad (\text{B.32})$$

where in the second step we took advantage of the identities

$$d^{adc} f^{cdb} = 0 , \quad f^{adc} f^{cdb} = -\text{tr}_{\text{adj}} T^a T^b = -N \delta^{ab} . \quad (\text{B.33})$$

In momentum space, we have to compute

$$\mathcal{W}_4(p) = \text{Diagram: a circle with a wavy line on the top side, and two external lines on the left and right. The left line is labeled '1' and '3', and the right line is labeled '2' and '6'.} \quad (\text{B.34})$$

which has the general form (B.16). Again, the θ -factors of the vertices saturate the integrations over θ_3 and $\bar{\theta}_4$, while the gluon propagator sets θ_6 and $\bar{\theta}_6$ equal to θ_5 and $\bar{\theta}_5$. The remaining Grassmann integrations are as in (B.26), but now with

$$\begin{aligned}\tilde{\mathfrak{D}}_4 &= \exp \left(-\theta_5(k_{53} + k_{45} + k_{46} + k_{62})\bar{\theta}_5 + 2\theta_5 k_{53}\bar{\theta}_3 + 2\theta_4(k_{45} + k_{46})\bar{\theta}_5 + 2\theta_4 k_{43}\bar{\theta}_3 \right) \\ &= \exp \left(-2\theta_5 p \bar{\theta}_5 - 2\theta_5 k_{53}\bar{\theta}_{53} - 2\theta_4 k_{43}\bar{\theta}_{53} \right)\end{aligned}\quad (\text{B.35})$$

where in the second step we used momentum conservation. The Grassmann integrations yield $\mathcal{Z}_4(p, k) = p^2 k_{43}^2$. This factor cancels one external and one internal propagator in \mathcal{Y}_4 and we remain with

$$\mathcal{W}_4(p) = \frac{1}{p^2} \text{ (diagram: a circle with two vertices, one on the left and one on the right, connected by a wavy line) } . \quad (\text{B.36})$$

Thus, the momentum space contribution corresponding to (B.32) is

$$\mathcal{W}_4^{ab}(p) = -4g_0^4 N(2N - N_f) \frac{1}{p^2} \text{ (diagram: a circle with two vertices, one on the left and one on the right, connected by a wavy line) } \delta^{ab} . \quad (\text{B.37})$$

We now consider the diagram

$$\begin{aligned}W_5^{ab}(x) &\equiv \text{ (diagram: a circle with two vertices, one on the left and one on the right, connected by a wavy line) } \\ &= -\frac{1}{2}(\sqrt{2}g_0)^2(2g_0)^2(T^a T^b)^{cd} (N_f \text{tr} T^c T^d - \text{tr}_{\text{adj}} T^c T^d) W_5(x) \\ &= 2g_0^4 N(2N - N_f) W_5(x) \delta^{ab} .\end{aligned}\quad (\text{B.38})$$

In momentum space, we have to compute

$$\mathcal{W}_5(p) = \text{ (diagram: a circle with two vertices, one on the left and one on the right, connected by a wavy line) } \quad (\text{B.39})$$

which again has the form (B.16) with

$$\begin{aligned}\tilde{\mathfrak{D}}_5 &= \exp \left(-2\theta_5(p + k_{53})\bar{\theta}_5 + 2\theta_5 k_{53}\bar{\theta}_3 - 2\theta_4 k_{53}\bar{\theta}_3 + 2\theta_4 k_{53}\bar{\theta}_5 \right) \\ &= \exp \left(-2\theta_5 p \bar{\theta}_5 + 2\theta_5 k_{53}\bar{\theta}_{35} - 2\theta_4 k_{53}\bar{\theta}_{35} \right) .\end{aligned}\quad (\text{B.40})$$

The Grassmann integration leads to $\mathcal{Z}_5(p, k) = p^2 k_{53}^2$, which cancels one external and one internal propagator in \mathcal{Y}_5 . We then remain with

$$\mathcal{W}_5(p) = \frac{1}{p^2} \text{ (diagram: a circle with two vertices, one on the left and one on the right, connected by a wavy line) } . \quad (\text{B.41})$$

Using this in (B.38), we find that the total diagram in momentum space is given by

$$\mathcal{W}_5^{ab}(p) = 2g_0^4 N(2N - N_f) \frac{1}{p^2} \text{ (tadpole diagram) } \delta^{ab} . \quad (\text{B.42})$$

Finally, we consider the diagram

$$\begin{aligned} W_6^{ab}(x) &\equiv \text{ (diagram: a horizontal line with wavy ends, a dashed loop on top, and arrows on the line and loop) } \\ &= 2 \times \left(-\frac{1}{2}\right)^2 (2g_0)^4 (T^a T^b)^{cd} (N_f \text{tr} T^c T^d - \text{tr}_{\text{adj}} T^c T^d) W_6(x) \\ &= -4g_0^2 N(2N - N_f) W_6(x) \delta^{ab} . \end{aligned} \quad (\text{B.43})$$

In momentum space, we have to compute

$$\mathcal{W}_6(p) = \text{ (diagram: a horizontal line with wavy ends, a loop on top with internal lines 5 and 6, and external lines 1, 3, 4, 2) } \quad (\text{B.44})$$

which, once again, is of the form (B.16) with

$$\begin{aligned} \tilde{\mathcal{D}}_6 &= \exp \left(-\theta_3(p + k_{56} + k_{65} + k_{34}) \bar{\theta}_3 - \theta_4(p + k_{56} + k_{65} + k_{34}) \bar{\theta}_4 \right. \\ &\quad \left. + 2\theta_3(k_{34} + k_{56}) \bar{\theta}_4 + 2\theta_4 k_{65} \bar{\theta}_3 \right) \\ &= \exp \left(-2\theta_3(k_{34} + k_{56}) \bar{\theta}_3 + 2\theta_4(k_{34} + k_{56}) \bar{\theta}_4 + 2\theta_4 k_{65} \bar{\theta}_3 \right) , \end{aligned} \quad (\text{B.45})$$

having used momentum conservation in the second step. The Grassmann integral we have to compute in this case is

$$\mathcal{Z}_6(p, k) = \int d^2\theta_3 d^2\bar{\theta}_2 d^2\theta_4 d^2\bar{\theta}_4 \tilde{\mathcal{D}}_6 . \quad (\text{B.46})$$

Integrating over $\bar{\theta}_4$ produces a factor of $(k_{34} + k_{56})^2 \theta_{34}^2$ which sets $\theta_4 = \theta_3$, so that in the end we remain with

$$\mathcal{Z}_6(p, k) = (k_{34} + k_{56})^2 \int d^2\theta_3 d^2\bar{\theta}_3 \exp(-2\theta_3 p \bar{\theta}_3) = (k_{34} + k_{56})^2 p^2 \sim 2(k_{34} \cdot k_{56}) p^2 . \quad (\text{B.47})$$

The last step follows from the fact that when we integrate this expression over momenta, both the k_{34}^2 and the k_{56}^2 terms, canceling the corresponding propagator, give rise to tadpole-like integrals, which vanish in dimensional regularization. The symmetry of the diagram under $k_{56} \leftrightarrow -k_{65}$ allows us to rewrite the above result as

$$\mathcal{Z}_6(p, k) = (k_{34} \cdot (k_{56} - k_{65})) p^2 = (k_{34} \cdot k_{35}) p^2 = \frac{1}{2} (p^2 - k_{34}^2 - k_{35}^2) p^2 \sim \frac{1}{2} (p^2 - k_{35}^2) p^2 , \quad (\text{B.48})$$

where again we discarded the tadpole originating from k_{34}^2 . The first term cancels the two external propagators of \mathcal{Y}_6 , while the second term cancels one external and one internal propagator. Using the graphical notation of Appendix A, we can write

$$\mathcal{W}_6(p) = \frac{1}{2} \left[\text{diagram 1} - \frac{1}{p^2} \text{diagram 2} \right], \quad (\text{B.49})$$

so that, from (B.43) we see that the total diagram in momentum space is

$$\mathcal{W}_6^{ab}(p) = -2g_0^4 N(2N - N_f) \left[\text{diagram 1} - \frac{1}{p^2} \text{diagram 2} \right] \delta^{ab}. \quad (\text{B.50})$$

Summing the three diagrams (B.37), (B.42) and (B.50), a simplification takes place and we are left with

$$\sum_{I=4}^6 \mathcal{W}_I^{ab}(p) = -2g_0^4 N(2N - N_f) \text{diagram 1} \delta^{ab}. \quad (\text{B.51})$$

Taking the Fourier transform via (A.25d), we then have

$$\sum_{I=4}^6 W_I^{ab}(x) = \left(\frac{g_0^2}{8\pi^2} \right)^2 N(2N - N_f) \frac{\Gamma^2(1 - \epsilon)}{4\epsilon^2(1 - 2\epsilon)(1 + \epsilon)} (\pi x^2)^{2\epsilon} \Delta(x) \delta^{ab}. \quad (\text{B.52})$$

If we include also the $W_3^{ab}(x)$ diagram given in (B.29), we obtain the two-loop irreducible corrections to the propagator:

$$\sum_{I=3}^6 W_I^{ab}(x) \equiv v_{2,2} \Delta(x) \delta^{ab} \quad (\text{B.53})$$

with

$$v_{2,2} = - \left(\frac{g_0^2}{8\pi^2} \right)^2 \left[3 \zeta(3) \left(\frac{N_f}{2N} + N^2 \right) - N(2N - N_f) \frac{\Gamma^2(1 - \epsilon)}{4\epsilon^2(1 - 2\epsilon)(1 + \epsilon)} \right] (\pi x^2)^{2\epsilon}, \quad (\text{B.54})$$

as reported in the formula (2.18) of the main text.

Irreducible diagrams: the $v_{4,2}$ part

We now evaluate the irreducible two-loop diagrams that give rise to the contribution (c) in Fig. 1. We start from the diagrams represented in Fig. 9. The first of these is

$$\begin{aligned} W_7^{a_1 a_2 b_1 b_2}(x) &\equiv \\ &\text{diagram} \\ &= 2 \times \left(-\frac{1}{2} \right) (\sqrt{2}g_0)^2 (2g_0)^2 (N_f \text{tr} T^c T^{a_2} T^{b_2} - \text{tr}_{\text{adj}} T^c T^{a_2} T^{b_2}) (T^c)^{a_1 b_1} W_7(x). \end{aligned} \quad (\text{B.55})$$

Using the relations (B.31), we find

$$W_7^{a_1 a_2 b_1 b_2}(x) = -2g_0^4 \left(i f^{ca_2 b_2} (N_f - 2N) + N_f d^{ca_2 b_2} \right) \left(-i f^{ca_1 b_1} \right) W_7(x) . \quad (\text{B.56})$$

Defining the tensor (see (2.21))

$$C_4^{(A) a_1 a_2 b_1 b_2} = -\frac{1}{N} f^{c a_1 b_1} f^{c a_2 b_2} , \quad (\text{B.57})$$

we can write

$$W_7^{a_1 a_2 b_1 b_2}(x) = -2g_0^4 \left(N(2N - N_f) C_4^{(A) a_1 a_2 b_1 b_2} + i N_f d^{a_2 b_2 c} f^{a_1 b_1 c} \right) W_7(x) . \quad (\text{B.58})$$

Note that the term proportional to $d^{a_2 b_2 c} f^{a_1 b_1 c}$ is actually anti-symmetric in (a_1, a_2) and in (b_1, b_2) , and thus it vanishes when we insert this sub-diagram in a chiral/anti-chiral correlator. Therefore in the following we discard this term.

In momentum space, we have to compute

$$\mathcal{W}_7(p) = \begin{array}{c} \begin{array}{c} \xrightarrow{1} \quad \quad \quad \xrightarrow{2} \\ \quad \quad \quad \uparrow \text{wavy} \quad \downarrow \\ \quad \quad \quad 5 \quad \quad \quad 6 \\ \quad \quad \quad \downarrow \text{wavy} \quad \uparrow \\ \quad \quad \quad 3 \quad \quad \quad 4 \\ \xrightarrow{1} \quad \quad \quad \xrightarrow{2} \end{array} \end{array} \quad (\text{B.59})$$

which has the canonical form (B.16). In this case we have

$$\begin{aligned} \tilde{\mathfrak{D}}_7 &= \exp \left(-\theta_6 (k_{63} + k_{46} + k_{15} + k_{52}) \bar{\theta}_6 + 2\theta_6 k_{63} \bar{\theta}_3 + 2\theta_4 k_{46} \bar{\theta}_6 + 2\theta_4 k_{43} \bar{\theta}_3 \right) \\ &= \exp \left(-2\theta_6 (k_{46} + k_{15}) \bar{\theta}_6 + 2\theta_6 k_{63} \bar{\theta}_3 + 2\theta_4 k_{46} \bar{\theta}_6 + 2\theta_4 k_{43} \bar{\theta}_3 \right) , \end{aligned} \quad (\text{B.60})$$

where in the second step we used momentum conservation. To perform the Grassmann integral

$$\mathcal{Z}_7(p, k) = \int d^2 \bar{\theta}_3 d^2 \theta_4 d^2 \theta_6 d^2 \bar{\theta}_6 \tilde{\mathfrak{D}}_7 , \quad (\text{B.61})$$

we use the formula

$$\int d^2 \theta_i d^2 \bar{\theta}_j d^2 \theta_k d^2 \bar{\theta}_l e^{2\theta_i A \bar{\theta}_j + 2\theta_i B \bar{\theta}_l + 2\theta_k C \bar{\theta}_l + 2\theta_k D \bar{\theta}_j} = A^2 C^2 + B^2 D^2 - \text{tr} (A D C B) \quad (\text{B.62})$$

where

$$\begin{aligned} \text{tr} (A D C B) &= \text{tr} \left(\sigma^\mu \bar{\sigma}^\nu \sigma^\lambda \bar{\sigma}^\rho \right) A_\mu D_\nu C_\lambda B_\rho \\ &= 2 A \cdot D C \cdot B - 2 A \cdot C D \cdot B + 2 A \cdot B D \cdot C - \varepsilon^{\mu\nu\lambda\rho} A_\mu D_\nu C_\lambda B_\rho . \end{aligned} \quad (\text{B.63})$$

In this way we obtain

$$\begin{aligned} \mathcal{Z}_7(p, k) &= (k_{46} + k_{15})^2 k_{43}^2 + k_{63}^2 k_{46}^2 + \text{tr} \left((k_{46} + k_{15}) k_{46} k_{43} k_{63} \right) \\ &= (k_{46} + k_{15})^2 k_{43}^2 + 2 \left((k_{46} + k_{15}) \cdot k_{46} \right) (k_{43} \cdot k_{63}) \\ &\quad - 2 \left((k_{46} + k_{15}) \cdot k_{43} \right) (k_{46} \cdot k_{63}) + 2 \left((k_{46} + k_{15}) \cdot k_{63} \right) (k_{43} \cdot k_{46}) , \end{aligned} \quad (\text{B.64})$$

In momentum space, we must compute

$$\mathcal{W}_8(p) = \begin{array}{c} \text{Diagram: A vertical wavy line connects two horizontal lines. The top horizontal line has endpoints 1 and 2, with a wavy line segment labeled 5. The bottom horizontal line has endpoints 1 and 2, with a wavy line segment labeled 6. A circular loop with arrows is attached to the wavy line segment 6, with vertices labeled 3 and 4.} \end{array} \quad (\text{B.70})$$

which again is of the form (B.16). In this case we have

$$\begin{aligned} \tilde{\mathfrak{D}} &= \exp \left(-\theta_6 (k_{15} + k_{16} + k_{52} + k_{63}) \bar{\theta}_6 + 2\theta_6 k_{63} \bar{\theta}_3 + 2\theta_4 k_{63} \bar{\theta}_3 \right) \\ &= \exp \left(-2\theta_6 p \bar{\theta}_6 + 2\theta_6 k_{63} \bar{\theta}_3 + 2\theta_4 k_{63} \bar{\theta}_3 \right) , \end{aligned} \quad (\text{B.71})$$

while the Grassmann integration yields $\mathcal{Z}_8(p, k) = p^2 k_{63}^2$. Inserting this into the momentum integrals, we remain with

$$\mathcal{W}_8(p) = p^2 \begin{array}{c} \text{Diagram: A circle with a vertical line through its center, and two dots on the horizontal line at the left and right edges.} \end{array} = 3 \begin{array}{c} \text{Diagram: A circle with a vertical line through its center, and two dots on the horizontal line at the left and right edges.} \end{array} + \dots \quad (\text{B.72})$$

where the last step follows from (A.20). Using this result, we find that the momentum space expression corresponding to $W_8^{a_1 a_2 b_1 b_2}(x)$ given in (B.69) is

$$\mathcal{W}_8^{a_1 a_2 b_1 b_2}(p) = 12g_0^4 N(2N - N_f) \begin{array}{c} \text{Diagram: A circle with a vertical line through its center, and two dots on the horizontal line at the left and right edges.} \end{array} C_4^{(A)a_1 a_2 b_1 b_2} + \dots \quad (\text{B.73})$$

where the dots stand for terms that vanish for $\epsilon \rightarrow 0$.

The third diagram we need to consider is

$$\begin{aligned} W_9^{a_1 a_2 b_1 b_2}(x) &\equiv \begin{array}{c} \text{Diagram: Two horizontal lines. The top line has endpoints a1 and b1, with a wavy line segment labeled x. The bottom line has endpoints a2 and b2, with a wavy line segment labeled x. A dashed circular loop with arrows is attached to the wavy line segment x, with vertices labeled 3 and 4.} \end{array} \\ &= 2 \times \left(-\frac{1}{2} \right)^2 (2g_0)^2 g_0^2 (N_f - 2N) (T^c)_{a_1 b_1} (T^c)_{a_2 b_2} W_9(x) \\ &= -2g_0^4 N(2N - N_f) C_4^{(A)a_1 a_2 b_1 b_2} W_9(x) . \end{aligned}$$

In momentum space, we have to compute

$$\mathcal{W}_9(p) = \begin{array}{c} \text{Diagram: Two horizontal lines. The top line has endpoints 1 and 2, with a wavy line segment labeled 3. The bottom line has endpoints 1 and 2, with a wavy line segment labeled 4. A circular loop with arrows is attached to the wavy line segment 4, with vertices labeled 5 and 6.} \end{array} \quad (\text{B.74})$$

which has again the form (B.16) with

$$\begin{aligned}\tilde{\mathcal{D}}_9 &= \exp\left(-\theta_3 (k_{13} + k_{32} + k_{56} + k_{65}) \bar{\theta}_3 - \theta_4 (k_{14} + k_{42} + k_{56} + k_{65}) \bar{\theta}_4 \right. \\ &\quad \left. + 2\theta_3 k_{56} \bar{\theta}_4 + 2\theta_4 k_{65} \bar{\theta}_3\right) \\ &= \exp\left(-2\theta_3 (k_{13} + k_{65}) \bar{\theta}_3 - 2\theta_4 (k_{14} + k_{56}) \bar{\theta}_4 + 2\theta_3 k_{56} \bar{\theta}_4 + 2\theta_4 k_{65} \bar{\theta}_3\right) .\end{aligned}\tag{B.75}$$

The Grassmann integration is carried out using (B.62) and gives

$$\mathcal{Z}_9(p, k) = (k_{13} + k_{65})^2 (k_{14} + k_{56})^2 + k_{56}^2 k_{65}^2 - \text{tr}((k_{13} + k_{65}) k_{65} (k_{14} + k_{56}) k_{56}) .\tag{B.76}$$

We expand the trace according to (B.63), and take into account the part proportional to the ε -tensor does not contribute. The terms proportional to k_{56}^2 and/or to k_{65}^2 , as well as the term $k_{13}^2 k_{14}^2$, are tadpole-like and vanish in dimensional regularization, and thus we remain with

$$\begin{aligned}\mathcal{Z}_9(p, k) &= 2k_{14}^2 (k_{65} \cdot k_{13}) + 2k_{13}^2 (k_{56} \cdot k_{14}) - 2(k_{13} \cdot k_{65})(k_{14} \cdot k_{56}) \\ &\quad + 2(k_{13} \cdot k_{56})(k_{14} \cdot k_{65}) + 2(k_{13} \cdot k_{14})(k_{56} \cdot k_{65}) .\end{aligned}\tag{B.77}$$

The diagram is symmetric under the exchange $k_{56} \leftrightarrow k_{65}$. Symmetrizing $\mathcal{Z}_9(p, k)$ with respect to this exchange, exploiting momentum conservation and discarding tadpole-like terms proportional to k_{56}^2 , k_{65}^2 or $k_{13}^2 k_{14}^2$ we can rewrite (B.77) as

$$\begin{aligned}\mathcal{Z}_9(p, k) &= -k_{14}^2 (k_{35} \cdot k_{13}) + k_{13}^2 (k_{64} \cdot k_{14}) - k_{64}^2 (k_{13} \cdot k_{14}) \\ &= \frac{1}{2} k_{14}^2 k_{32}^2 + \frac{1}{2} k_{13}^2 k_{42}^2 - \frac{1}{2} p^2 k_{64}^2 .\end{aligned}\tag{B.78}$$

The first two terms in the last expression give the same result and cancel two internal propagators, while the last term cancels one external and one internal propagator of \mathcal{Y}_9 . In the end, adopting the graphical notation of Appendix A, we have

$$\mathcal{W}_9(p) = \text{Diagram 1} - \frac{1}{2} p^2 \text{Diagram 2} = \text{Diagram 3} - \frac{3}{2} \text{Diagram 4} + \dots\tag{B.79}$$

where the second step follows from (A.23). Inserting this result in (B.74), we see that the momentum space expression corresponding to $W_9^{a_1 a_2 b_1 b_2}(x)$ is

$$\mathcal{W}_9^{a_1 a_2 b_1 b_2}(p) = g_0^4 N(2N - N_f) \left[-2 \text{Diagram 1} + 3 \text{Diagram 2} \right] C_4^{(A) a_1 a_2 b_1 b_2} + \dots .\tag{B.80}$$

Summing the three diagrams (B.68), (B.73) and (B.80), we find

$$\sum_{I=7}^9 \mathcal{W}_I^{a_1 a_2 b_1 b_2}(p) = g_0^4 N(2N - N_f) \left[7 \text{Diagram 1} - 2 \text{Diagram 2} \right] C_4^{(A) a_1 a_2 b_1 b_2} + \dots .\tag{B.81}$$

Performing the Fourier transform using (A.15) and (A.24), we finally obtain

$$\sum_{I=7}^9 W_I^{a_1 a_2 b_1 b_2}(x) = v_{4,2}^{(A)} \Delta(x)^2 C_4^{(A) a_1 a_2 b_1 b_2} + \dots\tag{B.82}$$

with

$$v_{4,2}^{(A)} = \left(\frac{g_0^2}{8\pi^2} \right)^2 N(2N - N_f) \left[\frac{21}{2} \zeta(3) + \frac{\Gamma^2(1 - \epsilon)}{4\epsilon^2(1 - 2\epsilon)(1 + \epsilon)} \right] (\pi x^2)^{2\epsilon} + \dots \quad (\text{B.83})$$

in agreement with the formula (2.20) of the main text.

The last two-loop diagram we have to compute is

$$\begin{aligned} W_{10}^{a_1 a_2 b_1 b_2}(x) &\equiv \quad (\text{B.84}) \\ &\quad \begin{array}{c} \begin{array}{ccc} \xrightarrow{\frac{a_1}{x}} & \text{---} & \xrightarrow{\frac{b_1}{0}} \\ \parallel & & \parallel \\ \text{---} & & \text{---} \\ \parallel & & \parallel \\ \xleftarrow{\frac{b_2}{0}} & \text{---} & \xleftarrow{\frac{a_2}{x}} \end{array} \\ \end{array} \\ &= \frac{2}{2!^2} (\sqrt{2}g_0)^4 (N_f \text{tr} T^{a_1} T^{b_1} T^{a_2} T^{b_2} - \text{tr}_{\text{adj}} T^{a_1} T^{b_1} T^{a_2} T^{b_2}) W_{10}(x) . \end{aligned}$$

This diagram was already computed in [15] in configuration space. For completeness we report here its evaluation in momentum space. Using the relation

$$\begin{aligned} \text{tr}_{\text{adj}} T^{a_1} T^{b_1} T^{a_2} T^{b_2} &= 2N \text{tr} T^{a_1} T^{b_1} T^{a_2} T^{b_2} + \frac{1}{2} (\delta^{a_1 b_1} \delta^{a_2 b_2} + \delta^{a_1 a_2} \delta^{b_1 b_2} + \delta^{a_1 b_2} \delta^{a_2 b_1}) \\ &\quad + \frac{iN}{4} (f^{a_1 b_1 c} d^{a_2 b_2 c} + f^{a_2 b_2 c} d^{a_1 b_1 c}) , \end{aligned} \quad (\text{B.85})$$

and introducing the tensor (see (2.24))

$$C_4^{(B) a_1 a_2 b_1 b_2} = -(2N - N_f) \text{tr} T^{a_1} T^{b_1} T^{a_2} T^{b_2} - \frac{1}{2} (\delta^{a_1 b_1} \delta^{a_2 b_2} + \delta^{a_1 a_2} \delta^{b_1 b_2} + \delta^{a_1 b_2} \delta^{a_2 b_1}) , \quad (\text{B.86})$$

we can rewrite (B.84) as

$$W_{10}^{a_1 a_2 b_1 b_2}(x) = 2g_0^4 \left[C_4^{(B) a_1 a_2 b_1 b_2} - \frac{iN}{4} (f^{a_1 b_1 c} d^{a_2 b_2 c} + f^{a_2 b_2 c} d^{a_1 b_1 c}) \right] W_{10}(x) . \quad (\text{B.87})$$

As noted after (B.58), the last two terms in the square brackets are anti-symmetric in (a_1, a_2) and (b_1, b_2) . Therefore they vanish when inserted in a chiral/anti-chiral two-point function and can be discarded. The momentum space diagram corresponding to $W_{10}(x)$ is

$$\mathcal{W}_{10}(p) = \quad (\text{B.88})$$

which has the form (B.16) with

$$\tilde{\mathcal{D}}_{10} = \exp(2\theta_4 k_{43} \bar{\theta}_3 + 2\theta_4 k_{45} \bar{\theta}_5 + 2\theta_6 k_{65} \bar{\theta}_5 + 2\theta_6 k_{63} \bar{\theta}_3) . \quad (\text{B.89})$$

where the last term follows from $\square_x \Delta(x) = -\delta^{(D)}(x)$. Using this relation and performing the Grassmann integrations over $\bar{\theta}_3$ and θ_4 , we get

$$\int d^2 \bar{\theta}_3 d^2 \theta_4 \left(e^{-2i\theta_4 \partial_{x_{43}} \bar{\theta}_3} \Delta(x_{43}) \right)^2 = 2 \partial_{x_{43}} \Delta(x_{43}) \cdot \partial_{x_{43}} \Delta(x_{43}) - 2 \Delta(x_{43}) \delta^{(D)}(x_{43}) . \quad (\text{C.3})$$

Inserting this expression in the integral (C.1), we see that the term proportional to the δ -function yields a tadpole-like contribution, which vanishes in dimensional regularization and thus can be discarded. We then remain with

$$\begin{aligned} I(x_1, x_2) &= 2 \int d^D x_3 d^D x_4 \Delta(x_{13}) \partial_{x_{43}} \Delta(x_{43}) \cdot \partial_{x_{43}} \Delta(x_{43}) \Delta(x_{42}) [\kappa(x_3) \kappa(x_4)]^{-\epsilon} \\ &= 8 \left(\frac{\Gamma(1-\epsilon)}{4\pi^{2-\epsilon}} \right)^4 (1-\epsilon)^2 \int d^D x_3 d^D x_4 \frac{[\kappa(x_3) \kappa(x_4)]^{-\epsilon}}{(x_{13}^2)^{1-\epsilon} (x_{43}^2)^{3-2\epsilon} (x_{42}^2)^{1-\epsilon}} , \end{aligned} \quad (\text{C.4})$$

where in the second step we used the explicit expression (2.7) of the scalar propagator.

To simplify the calculation, without any loss of generality, we set $R = 1$ and choose the point η_2 to be at the north pole on the sphere, namely $\eta_2 = (1, 0, \dots, 0)$. According to the stereographic projection (5.2), this corresponds to sending $x_2 \rightarrow \infty$. We therefore find

$$[\kappa(x_1) \kappa(x_2)]^{1-\epsilon} I(x_1, x_2) \stackrel{x_2 \rightarrow \infty}{\approx} 2^{2+3\epsilon} \left(\frac{\Gamma(1-\epsilon)}{4\pi^{2-\epsilon}} \right)^2 \left(\frac{x_1^2 + 1}{2} \right)^{1-\epsilon} Y(x_1^2) , \quad (\text{C.5})$$

where

$$Y(x_1^2) = \left(\frac{\Gamma(2-\epsilon)}{4\pi^{2-\epsilon}} \right)^2 \int d^D x_3 d^D x_4 \frac{1}{(x_{13}^2)^{1-\epsilon} (x_{43}^2)^{3-2\epsilon} (x_3^2 + 1)^\epsilon (x_4^2 + 1)^\epsilon} . \quad (\text{C.6})$$

It is not difficult to realize that this function is regular for $x_1^2 \rightarrow 0$ and satisfies the following differential equation

$$\square_{x_1} Y(x_1^2) = -\frac{\Gamma(2-\epsilon)}{4\pi^{2-\epsilon}} (1-\epsilon) (x_1^2 + 1)^{-\epsilon} \int d^D x_4 \frac{1}{(x_{41}^2)^{3-2\epsilon} (x_4^2 + 1)^\epsilon} . \quad (\text{C.7})$$

We rewrite the right hand side of (C.7) using the Schwinger parametrization

$$\frac{1}{(x^2 + a^2)^\alpha} = \frac{1}{\Gamma(\alpha)} \int_0^\infty ds s^{\alpha-1} e^{-s(x^2 + a^2)} , \quad (\text{C.8})$$

and, after computing the resulting Gaussian integral over x_4 , we obtain

$$\begin{aligned} \square_{x_1} Y(x_1^2) &= -\frac{\Gamma(2-\epsilon)}{8\Gamma(2-2\epsilon)\Gamma(\epsilon)} (x_1^2 + 1)^{-\epsilon} \int_0^\infty ds_1 \int_0^\infty ds_2 \frac{s_1^{-1+\epsilon} s_2^{2-2\epsilon}}{(s_1 + s_2)^{2-\epsilon}} e^{-s_1 \frac{s_1 + s_2 (x_1^2 + 1)}{s_1 + s_2}} \\ &= -\frac{\Gamma(2-\epsilon)}{8\Gamma(2-2\epsilon)\Gamma(\epsilon)} (x_1^2 + 1)^{-\epsilon} \int_0^\infty dt t^{-2+\epsilon} (1+t)^{-1+\epsilon} \frac{1}{t + x_1^2 + 1} , \end{aligned} \quad (\text{C.9})$$

where the last step follows from changing the integration variable according to $s_1 \rightarrow t s_2$ and performing the resulting integral over s_2 . With the further change of integration variable $t \rightarrow \frac{1-y}{y}$, we can rewrite the t -integral as

$$\int_0^1 dy y^{2-2\epsilon} (1-y)^{-2+\epsilon} \frac{1}{1 + x_1^2 y} = \frac{\Gamma(3-2\epsilon)\Gamma(\epsilon-1)}{\Gamma(2-\epsilon)} {}_2F_1(1, 3-2\epsilon, 2-\epsilon; -x_1^2) . \quad (\text{C.10})$$

Substituting this into (C.9), in the end we find

$$\square_{x_1} Y(x_1^2) = \frac{1}{4} (x_1^2 + 1)^{-\epsilon} {}_2F_1(1, 3 - 2\epsilon, 2 - \epsilon; -x_1^2) = \frac{x_1^2 + 2}{8(x_1^2 + 1)^2} + O(\epsilon) . \quad (\text{C.11})$$

The general solution to this differential equation which is regular for $x_1^2 \rightarrow 0$ is

$$Y(x_1^2) = \frac{1}{32} (c_0 + \ln(x_1^2 + 1) + O(\epsilon)) \quad (\text{C.12})$$

with c_0 an arbitrary constant. To fix it, we examine $Y(x_1^2)$ for $x_1 \rightarrow \infty$, corresponding to the short-distance limit on the sphere in which also η_1 is sent to the north pole. In this limit the leading contribution to (C.6) comes from large x_3^2 and x_4^2 , allowing us to replace the scaling factors $(1 + x_i^2)^\epsilon$ with $(x_i^2)^\epsilon$. This leads to

$$\begin{aligned} Y(x_1^2) &\stackrel{x_1^2 \rightarrow \infty}{\simeq} \left(\frac{\Gamma(1 - \epsilon)}{4\pi^{2-\epsilon}} \right)^2 (1 - \epsilon)^2 \int d^{4-2\epsilon} x_3 \frac{1}{(x_{13}^2)^{1-\epsilon} (x_3^2)^\epsilon} \int d^{4-2\epsilon} x_4 \frac{1}{(x_{34}^2)^{3-2\epsilon} (x_4^2)^\epsilon} \\ &\simeq -\frac{(x_1^2)^{-\epsilon}}{32\epsilon(1-2\epsilon)} \simeq \frac{1}{32} \left(-\frac{1}{\epsilon(1-2\epsilon)} + \ln x_1^2 + O(\epsilon) \right) . \end{aligned} \quad (\text{C.13})$$

Comparing with (C.12) in the limit $x_1^2 \rightarrow \infty$, we deduce that

$$c_0 = -\frac{1}{\epsilon(1-2\epsilon)} . \quad (\text{C.14})$$

Therefore, we can write

$$Y(x_1^2) = -\frac{(x_1^2 + 1)^{-\epsilon}}{32\epsilon(1-2\epsilon)} + O(\epsilon) . \quad (\text{C.15})$$

The x_2 -dependence can be easily restored by noticing that $\eta_{12}^2 \simeq 4/(x_1^2 + 1)$ at large x_2 ; this means that at finite x_2 , the variable x_1^2 must be replaced by

$$r_{12}^2 = \frac{4}{\eta_{12}^2} - 1 \quad (\text{C.16})$$

and the function $Y(x_1^2)$ by

$$Y(r_{12}^2) = -\frac{2^{-2\epsilon} (\eta_{12}^2)^\epsilon}{32\epsilon(1-2\epsilon)} + O(\epsilon) . \quad (\text{C.17})$$

We now use this information in (C.5) and find

$$\begin{aligned} W_{1S}(\eta_{12}) &\equiv [\kappa(x_1) \kappa(x_2)]^{1-\epsilon} I(x_1, x_2) \\ &= 2^{3+2\epsilon} \frac{\Gamma(1-\epsilon)}{4\pi^{2-\epsilon}} \Delta_S(\eta_{12}) Y(r_{12}^2) \\ &= \frac{(\pi\eta_{12}^2)^\epsilon \Gamma(-\epsilon)}{(4\pi)^2 (1-2\epsilon)} \Delta_S(\eta_{12}) + O(\epsilon) , \end{aligned} \quad (\text{C.18})$$

where we used (5.4) in the second line, and (C.17) in the final step. This is the formula (5.18) of the main text. We have also computed the $O(\epsilon)$ terms, finding

$$W_{1S}(\eta_{12}) = \frac{(\pi\eta_{12}^2)^\epsilon \Gamma(-\epsilon)}{(4\pi)^2 (1-2\epsilon)} \Delta_S(\eta_{12}) \left(1 - \epsilon^2 \phi(r_{12}^2) + O(\epsilon^3) \right) \quad (\text{C.19})$$

with

$$\phi(x^2) = \text{Li}_2(-x^2) + \frac{1}{2} \ln^2(x^2 + 1) + \frac{\ln(x^2 + 1)}{x^2} + \frac{\pi^2}{6} . \quad (\text{C.20})$$

It is straightforward to verify that $\phi(x^2)$ vanishes at large x^2 and approaches a finite value for $x^2 \rightarrow 0$.

References

- [1] J. K. Erickson, G. W. Semenoff, and K. Zarembo, *Wilson loops in $N=4$ supersymmetric Yang-Mills theory*, *Nucl. Phys.* **B582** (2000) 155–175, [[hep-th/0003055](#)].
- [2] D. E. Berenstein, R. Corrado, W. Fischler, and J. M. Maldacena, *The Operator product expansion for Wilson loops and surfaces in the large N limit*, *Phys. Rev.* **D59** (1999) 105023, [[hep-th/9809188](#)].
- [3] N. Drukker and D. J. Gross, *An Exact prediction of $N=4$ SUSYM theory for string theory*, *J. Math. Phys.* **42** (2001) 2896–2914, [[hep-th/0010274](#)].
- [4] G. W. Semenoff and K. Zarembo, *More exact predictions of SUSYM for string theory*, *Nucl. Phys.* **B616** (2001) 34–46, [[hep-th/0106015](#)].
- [5] F. Fucito, J. F. Morales, and R. Poghossian, *Wilson loops and chiral correlators on squashed spheres*, *JHEP* **11** (2015) 064, [[arXiv:1507.05426](#)].
- [6] V. Pestun, *Localization of gauge theory on a four-sphere and supersymmetric Wilson loops*, *Commun.Math.Phys.* **313** (2012) 71–129, [[arXiv:0712.2824](#)].
- [7] R. Andree and D. Young, *Wilson Loops in $N=2$ Superconformal Yang-Mills Theory*, *JHEP* **09** (2010) 095, [[arXiv:1007.4923](#)].
- [8] M. Baggio, V. Niarchos, and K. Papadodimas, *Exact correlation functions in $SU(2)\mathcal{N}=2$ superconformal QCD*, *Phys. Rev. Lett.* **113** (2014), no. 25 251601, [[arXiv:1409.4217](#)].
- [9] M. Baggio, V. Niarchos, and K. Papadodimas, *On exact correlation functions in $SU(N)\mathcal{N}=2$ superconformal QCD*, *JHEP* **11** (2015) 198, [[arXiv:1508.03077](#)].
- [10] E. Gerchkovitz, J. Gomis, N. Ishtiaque, A. Karasik, Z. Komargodski, and S. S. Pufu, *Correlation Functions of Coulomb Branch Operators*, *JHEP* **01** (2017) 103, [[arXiv:1602.05971](#)].
- [11] M. Baggio, V. Niarchos, K. Papadodimas, and G. Vos, *Large- N correlation functions in $\mathcal{N}=2$ superconformal QCD*, [[arXiv:1610.07612](#)].
- [12] D. Rodriguez-Gomez and J. G. Russo, *Large N Correlation Functions in Superconformal Field Theories*, *JHEP* **06** (2016) 109, [[arXiv:1604.07416](#)].
- [13] D. Rodriguez-Gomez and J. G. Russo, *Operator Mixing in Large N Superconformal Field Theories on S^4 and Correlators with Wilson loops*, [[arXiv:1607.07878](#)].
- [14] M. Baggio, V. Niarchos, and K. Papadodimas, *tt^* equations, localization and exact chiral rings in $4d\mathcal{N}=2$ SCFTs*, *JHEP* **02** (2015) 122, [[arXiv:1409.4212](#)].
- [15] M. Billo, F. Fucito, A. Lerda, J. F. Morales, Ya. S. Stanev, and C. Wen, *Two-point Correlators in $N=2$ Gauge Theories*, *Nucl. Phys.* **B926** (2018) 427–466, [[arXiv:1705.02909](#)].
- [16] M. Billo, F. Galvagno, P. Gregori, and A. Lerda, *Correlators between Wilson loop and chiral operators in $\mathcal{N}=2$ conformal gauge theories*, *JHEP* **03** (2018) 193, [[arXiv:1802.09813](#)].

- [17] K. G. Chetyrkin and F. V. Tkachov, *Integration by Parts: The Algorithm to Calculate beta Functions in 4 Loops*, *Nucl. Phys.* **B192** (1981) 159–204.
- [18] A. Grozin, *Lectures on QED and QCD*, in *3rd Dubna International Advanced School of Theoretical Physics Dubna, Russia, January 29-February 6, 2005*, pp. 1–156, 2005. [[hep-ph/0508242](#)].
- [19] D. R. T. Jones, *Two Loop Diagrams in Yang-Mills Theory*, *Nucl. Phys.* **B75** (1974) 531.
- [20] D. M. Capper, D. R. T. Jones, and P. van Nieuwenhuizen, *Regularization by Dimensional Reduction of Supersymmetric and Nonsupersymmetric Gauge Theories*, *Nucl. Phys.* **B167** (1980) 479–499.
- [21] P. S. Howe and P. C. West, *The two loop beta function in models with extended rigid supersymmetry*, *Nucl. Phys.* **B242** (1984) 364–376.
- [22] V. A. Novikov, M. A. Shifman, A. I. Vainshtein, and V. I. Zakharov, *Exact Gell-Mann-Low Function of Supersymmetric Yang-Mills Theories from Instanton Calculus*, *Nucl. Phys.* **B229** (1983) 381–393.
- [23] V. A. Novikov, M. A. Shifman, A. I. Vainshtein, and V. I. Zakharov, *Beta Function in Supersymmetric Gauge Theories: Instantons Versus Traditional Approach*, *Phys. Lett.* **166B** (1986) 329–333, [*Yad. Fiz.* **43** (1986) 459].
- [24] N. Seiberg, *Supersymmetry and Nonperturbative beta Functions*, *Phys. Lett.* **B206** (1988) 75–80.
- [25] ALPHA Collaboration, S. Sint and P. Weisz, *The Running quark mass in the \overline{SF} scheme and its two loop anomalous dimension*, *Nucl. Phys.* **B545** (1999) 529–542, [[hep-lat/9808013](#)].
- [26] N. A. Nekrasov, *Seiberg-Witten prepotential from instanton counting*, *Adv. Theor. Math. Phys.* **7** (2003), no. 5 831–864, [[hep-th/0206161](#)].
- [27] N. Nekrasov and A. Okounkov, *Seiberg-Witten theory and random partitions*, *Prog. Math.* **244** (2006) 525–596, [[hep-th/0306238](#)].
- [28] E. Sysoeva, *Wilson loops and its correlators with chiral operators in $\mathcal{N} = 2, 4$ SCFT at large N* , *JHEP* **03** (2018) 155, [[arXiv:1712.10297](#)].
- [29] A. Bourget, D. Rodriguez-Gomez, and J. G. Russo, *Universality of Toda equation in $\mathcal{N} = 2$ superconformal field theories*, [[arXiv:1810.00840](#)].
- [30] S. L. Adler, *Massless, Euclidean Quantum Electrodynamics on the Five-Dimensional Unit Hypersphere*, *Phys. Rev.* **D6** (1972) 3445–3461.
- [31] S. L. Adler, *Massless electrodynamics on the five-dimensional unit hypersphere: an amplitude - integral formulation*, *Phys. Rev.* **D8** (1973) 2400–2418. [Erratum: *Phys. Rev.* **D15** (1977) 1803].
- [32] I. T. Drummond, *Dimensional Regularization of Massless Theories in Spherical Space-Time*, *Nucl. Phys.* **B94** (1975) 115–144.
- [33] I. T. Drummond, *Conformally Invariant Amplitudes and Field Theory in a Space-Time of Constant Curvature*, *Phys. Rev.* **D19** (1979) 1123.
- [34] I. T. Drummond and G. M. Shore, *Dimensional Regularization of Massless Quantum Electrodynamics in Spherical Space-Time. 1*, *Annals Phys.* **117** (1979) 89.